

# Decay-time dependent $CP$ -violation at Belle II

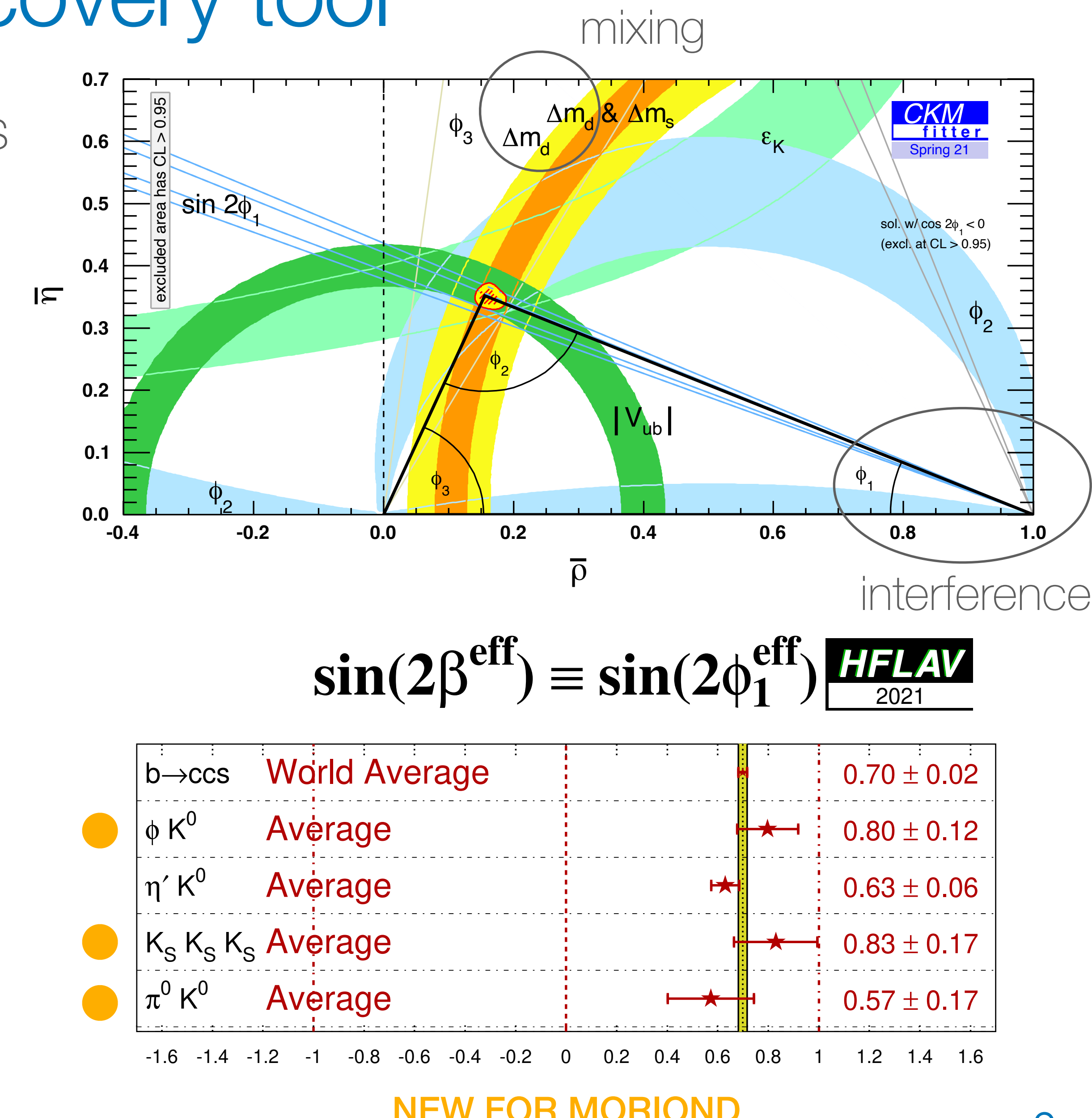
Michele Veronesi, on behalf of the Belle II collaboration  
Moriond EW, 18-25 March 2023

IOWA STATE  
UNIVERSITY



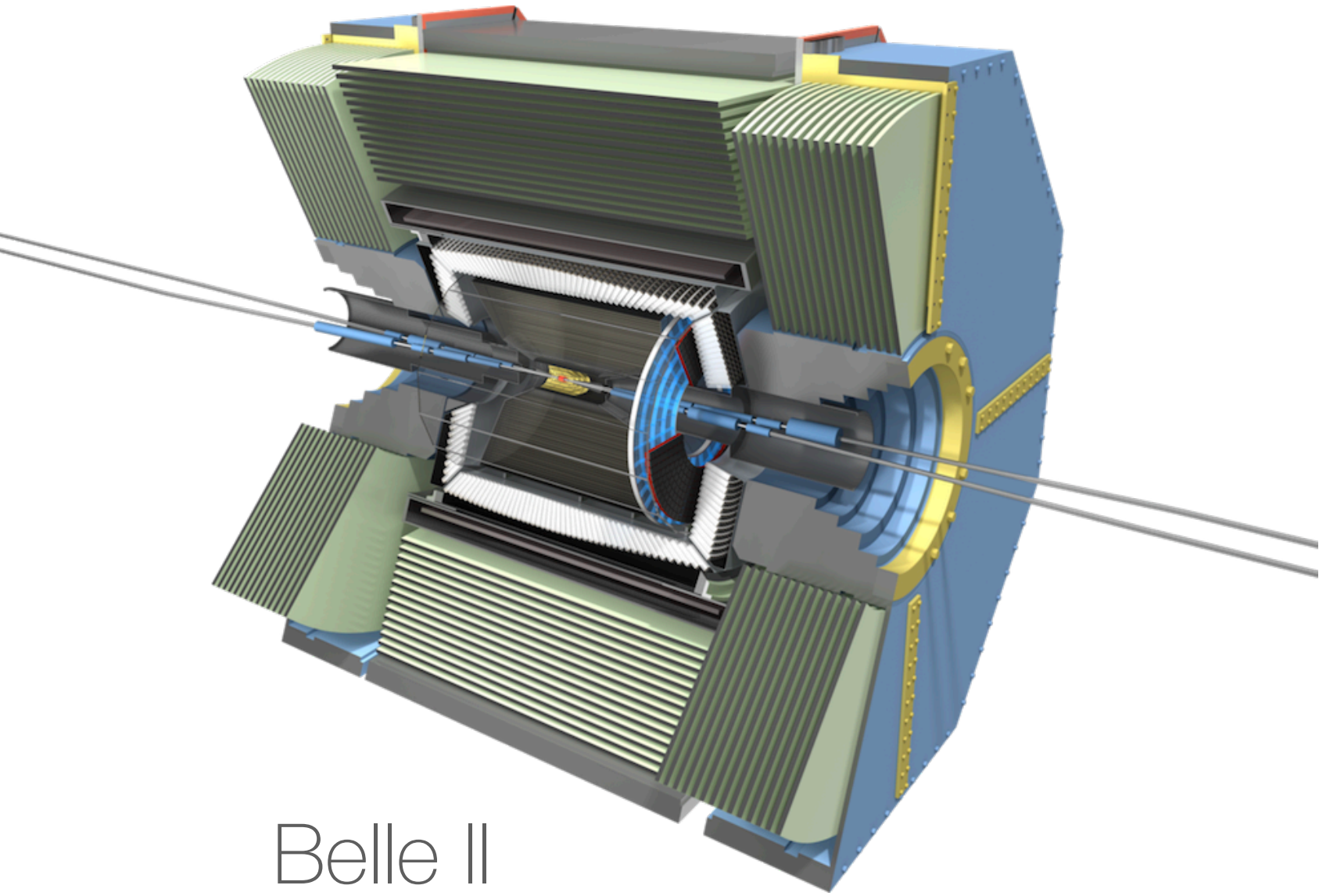
# Time-dependent CPV as discovery tool

- Measurements of  $\sin 2\phi_1$  in  $b \rightarrow q\bar{q}s$  transitions as a probe of beyond SM physics
  - ▶ Clean theory prediction ( $\sim$ few %)
  - ▶ Loop-suppressed, potentially affected by competing BSM amplitudes
- Experimentally challenging, due to
  - ▶ Small BF ( $\sim 10^{-6}$ ) and neutrals in the final state ( $K_s, \pi^0$ )
  - ▶ Sophisticated analysis techniques (tagging and  $\Delta t$  resolution)
- Validated with benchmark mixing and CPV analyses ( $B \rightarrow D^{(*)}\pi$  and  $B \rightarrow J/\psi K_s$ )

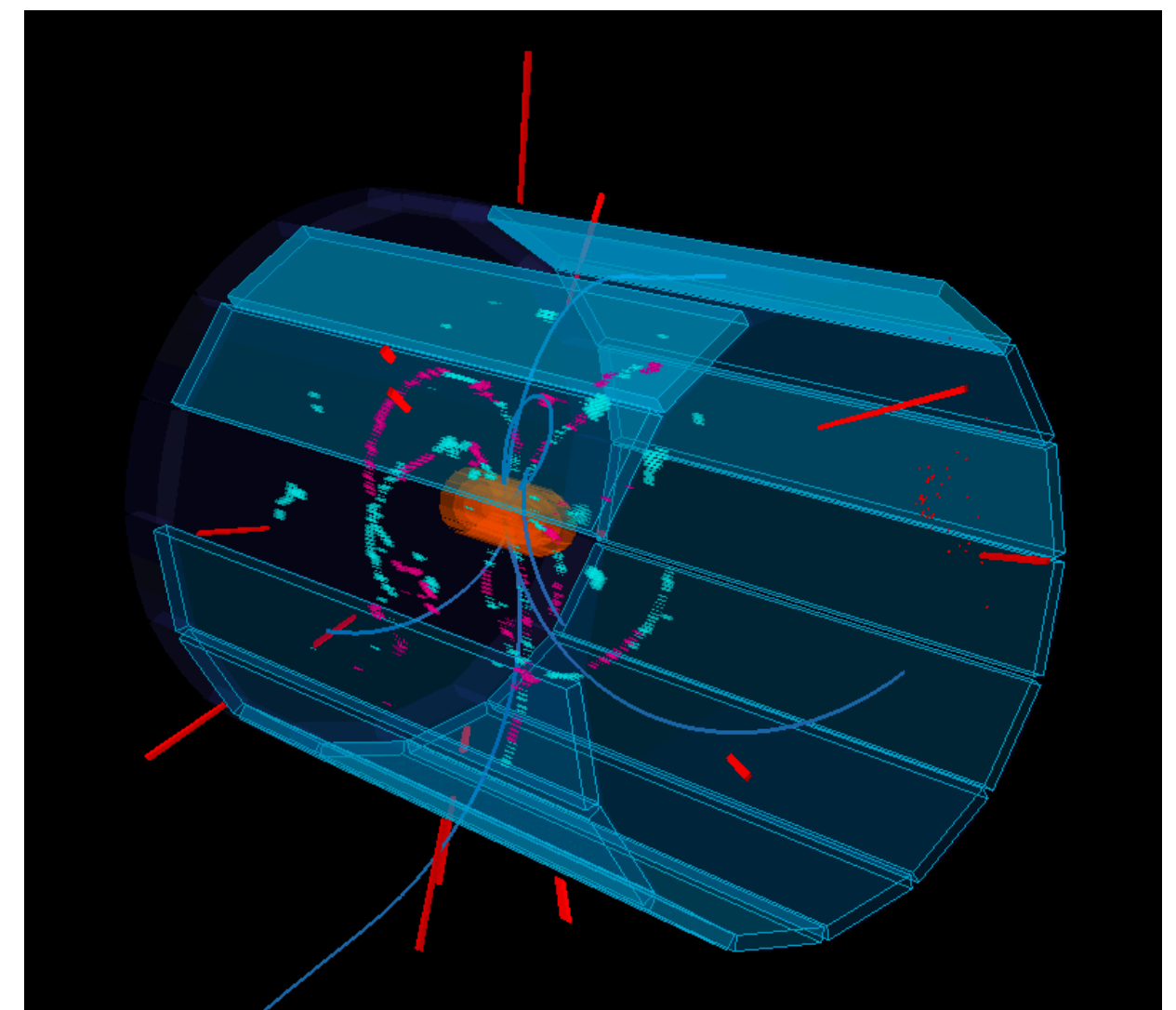


# Belle II at SuperKEKB

- Asymmetric  $e^+e^-$  collisions at the SuperKEKB accelerator complex in Japan
  - ▶ Recorded world's highest instantaneous luminosity ( $4.7 \times 10^{34} \text{ cm}^{-2}\text{s}^{-1}$ )
  - ▶ Collected  $362 \text{ fb}^{-1}$  dataset at the  $\Upsilon(4s)$  in 2019-22, corresponding to 387M  $B\bar{B}$  pairs
- Brand new detector, especially important for time-dependent measurements
  - ▶ Excellent vertex resolution from pixel and silicon vertex detectors
  - ▶ Efficient neutrals reconstruction ( $\pi^0, K_s$ ) and  $K/\pi$  separation

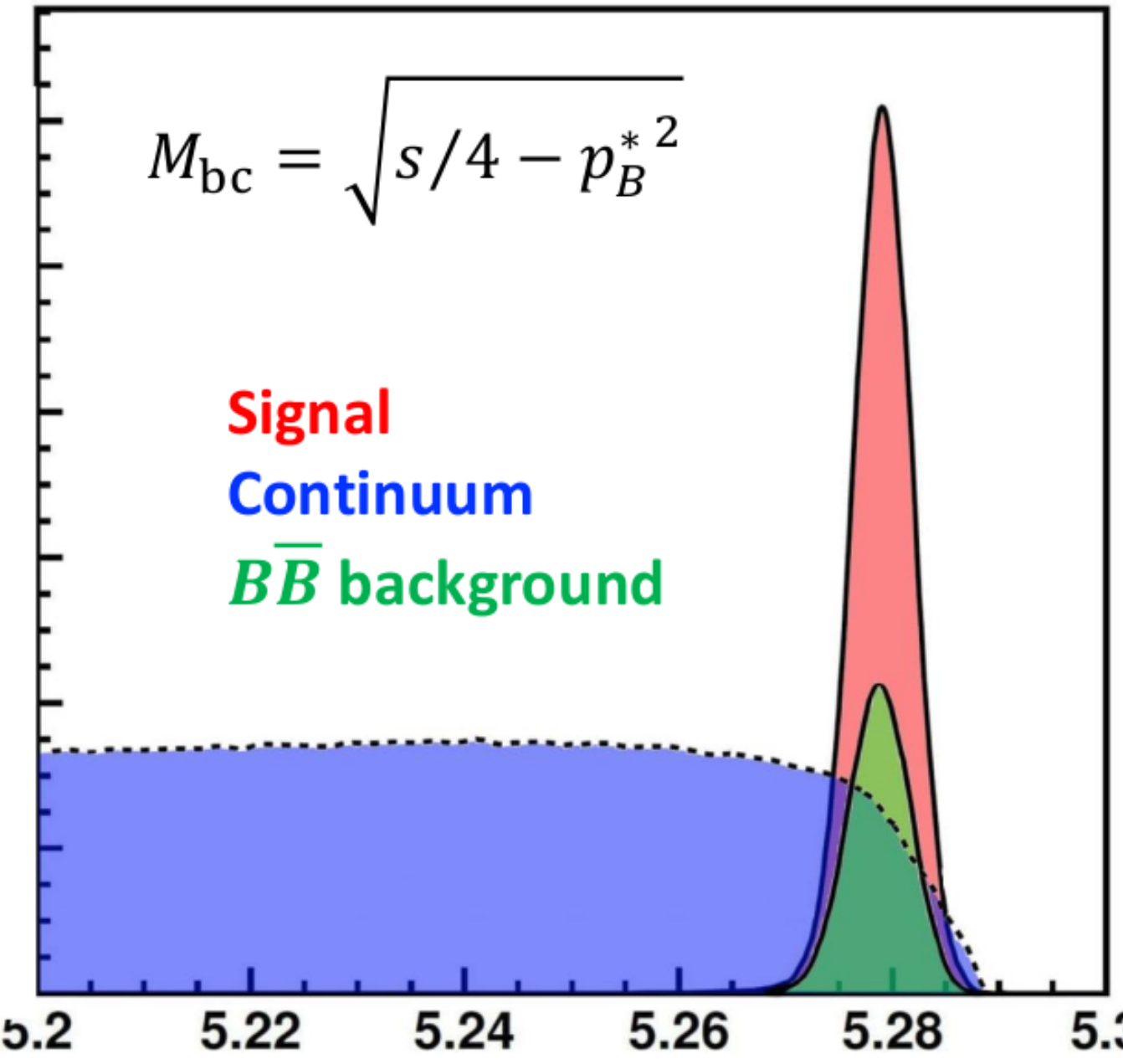


Belle II

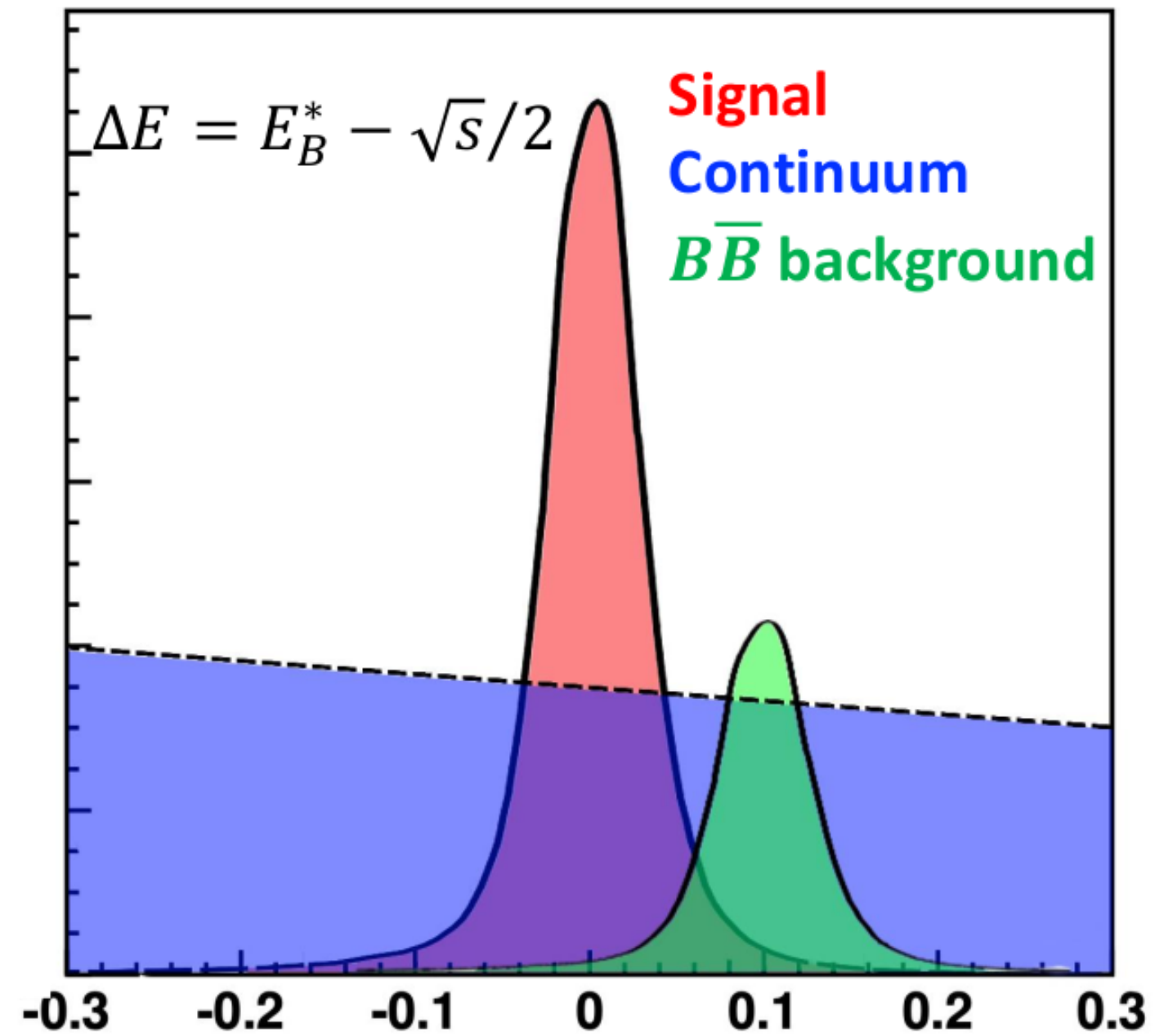


$e^+e^-$  collision

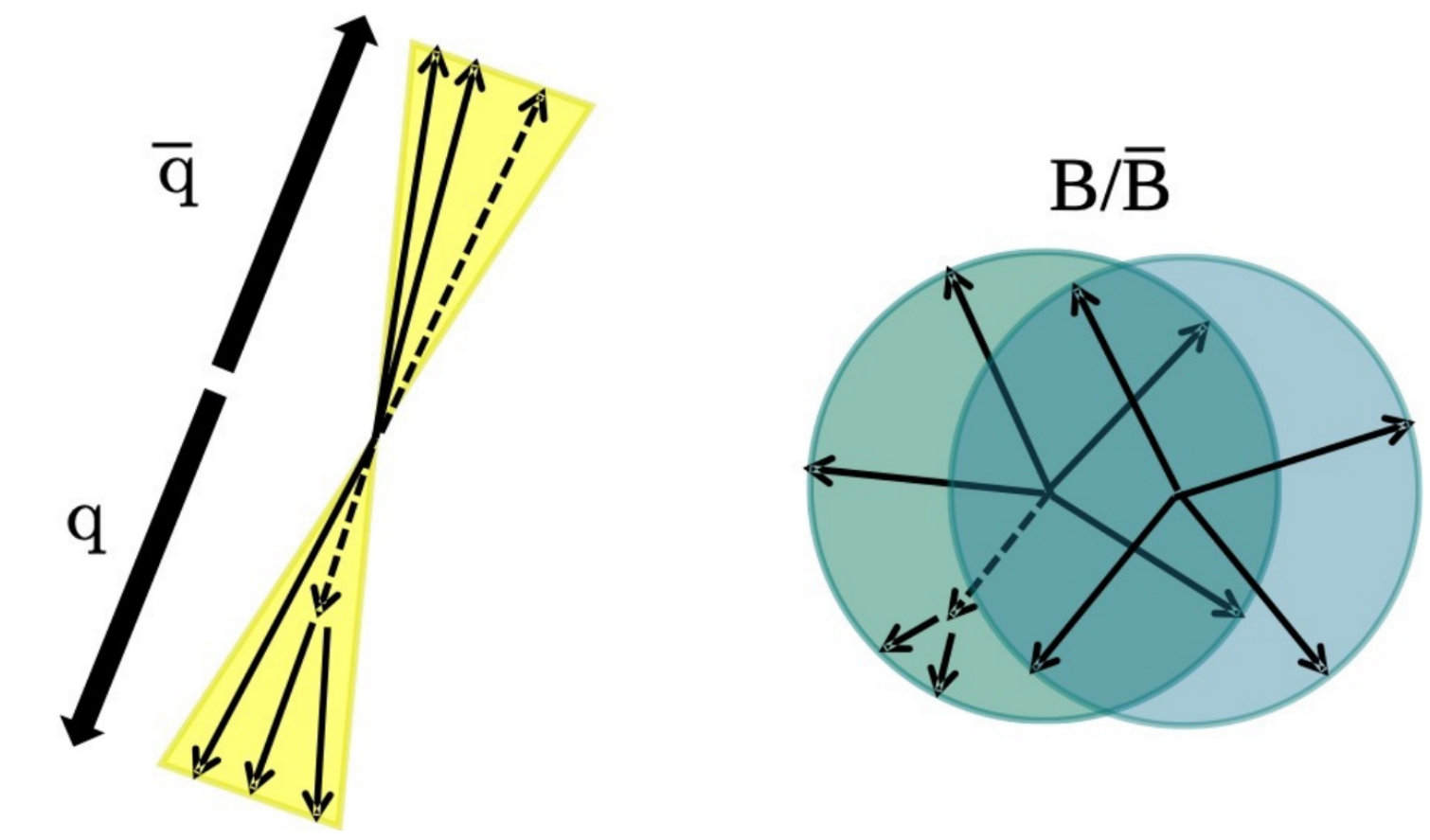
# B-factory analysis 101



Beam-constrained mass [GeV/c<sup>2</sup>]



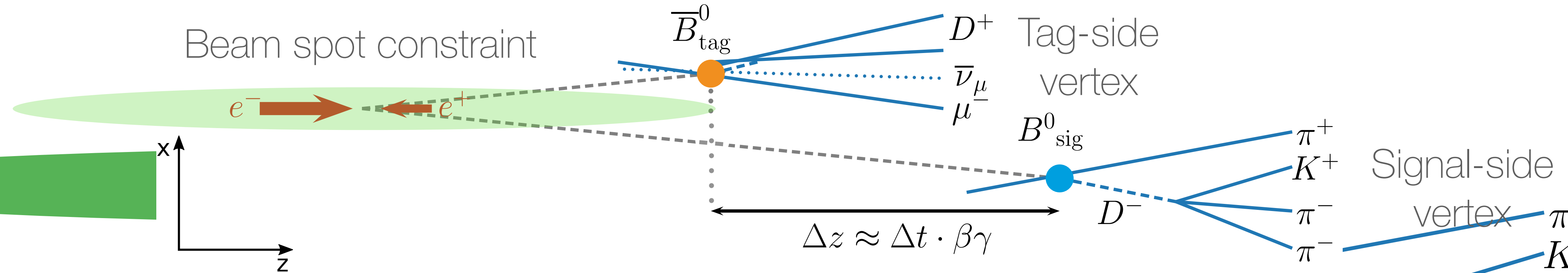
Energy difference [GeV]



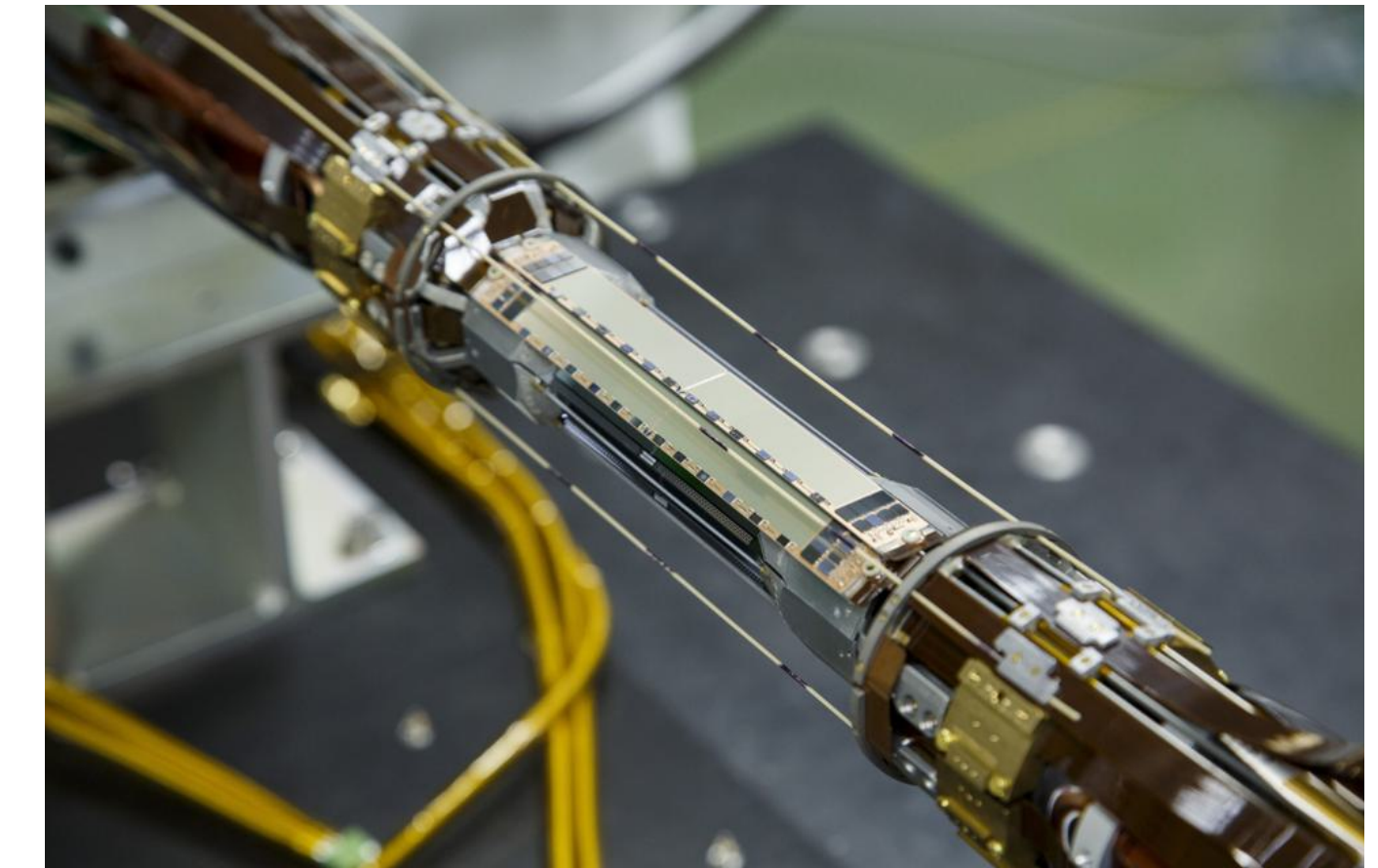
Event shape

- High resolution (~2-10 MeV) high-level analysis variables ( $M_{bc}$ ,  $\Delta E$ ), separating signal from backgrounds, using to the knowledge of beam energy
- Several event shape variables exploiting the correlations in  $e^+e^-$  collision

# Time measurement

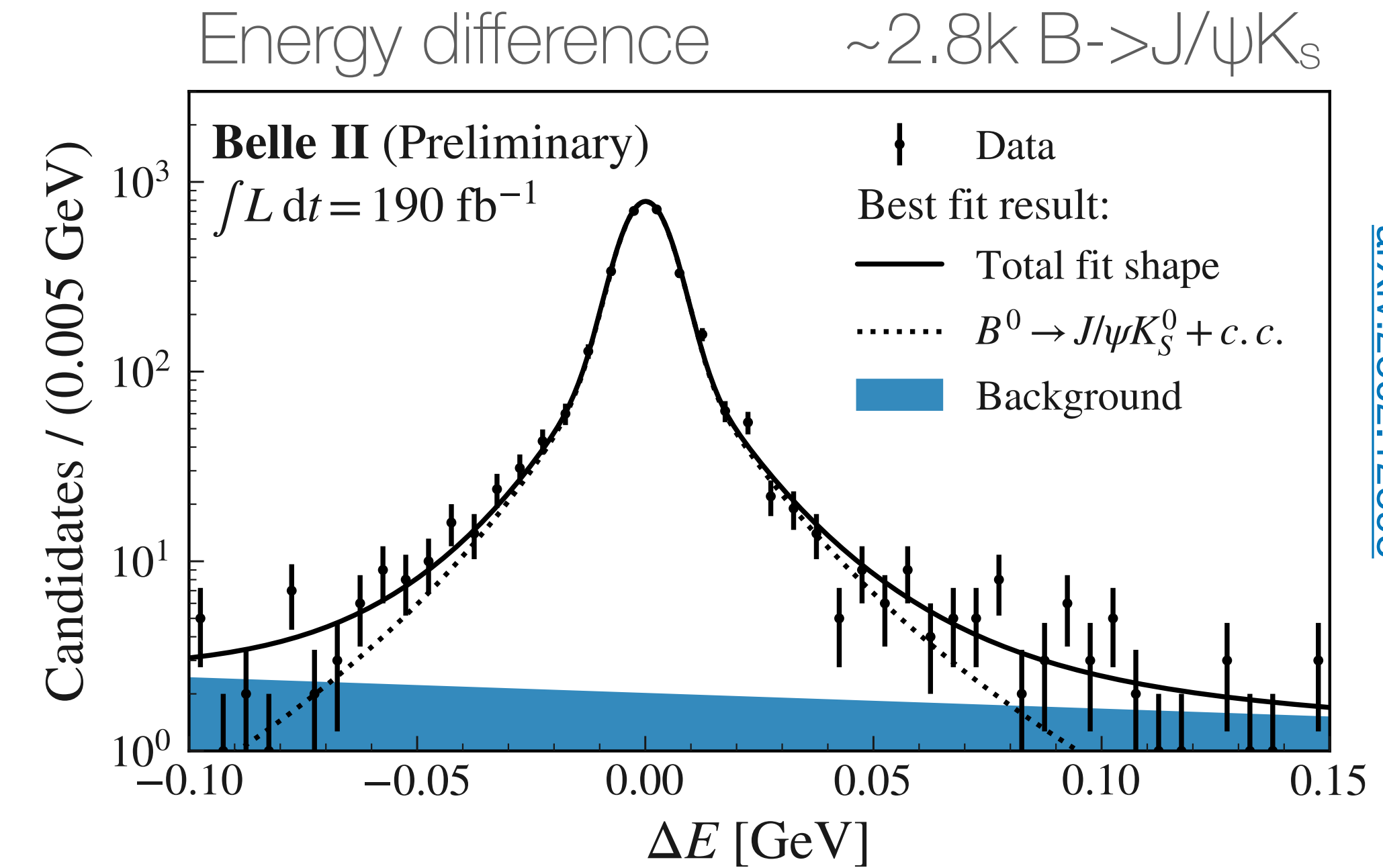
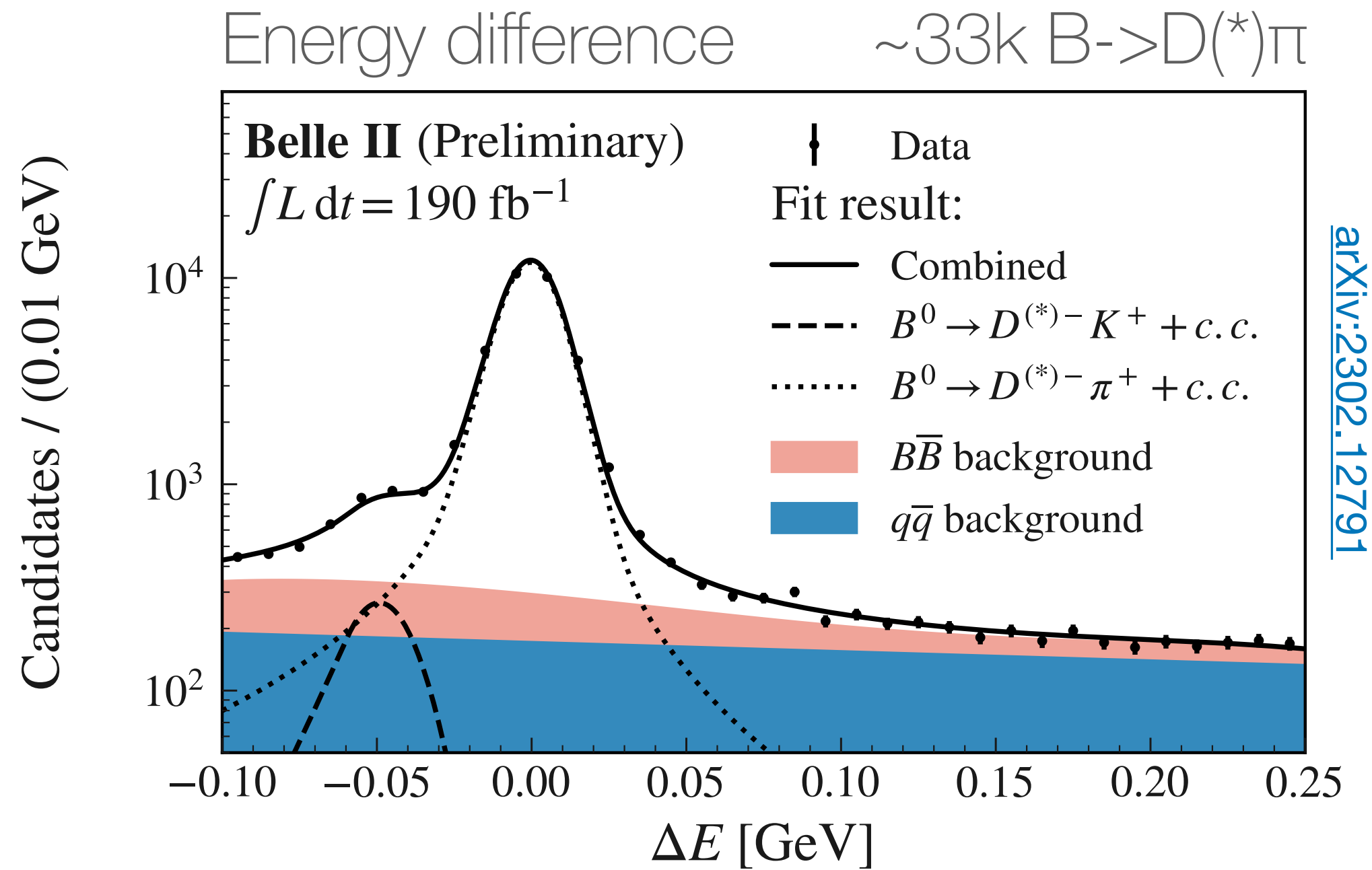


- Measuring the time difference  $\Delta t$  of coherently produced  $B\bar{B}$  pairs from the decay of a  $\Upsilon(4S)$ , boosted along  $z$
- Improved vertex resolution from pixel in spite of lower boost
  - ▶ Belle:  $\beta\gamma=0.43$ ,  $\Delta z \approx 200\mu\text{m}$  → Belle II:  $\beta\gamma=0.29$ ,  $\Delta z \approx 130\mu\text{m}$
- Enhanced  $\Delta t$  resolution from the beam spot profile in combination with the new nano-beam scheme



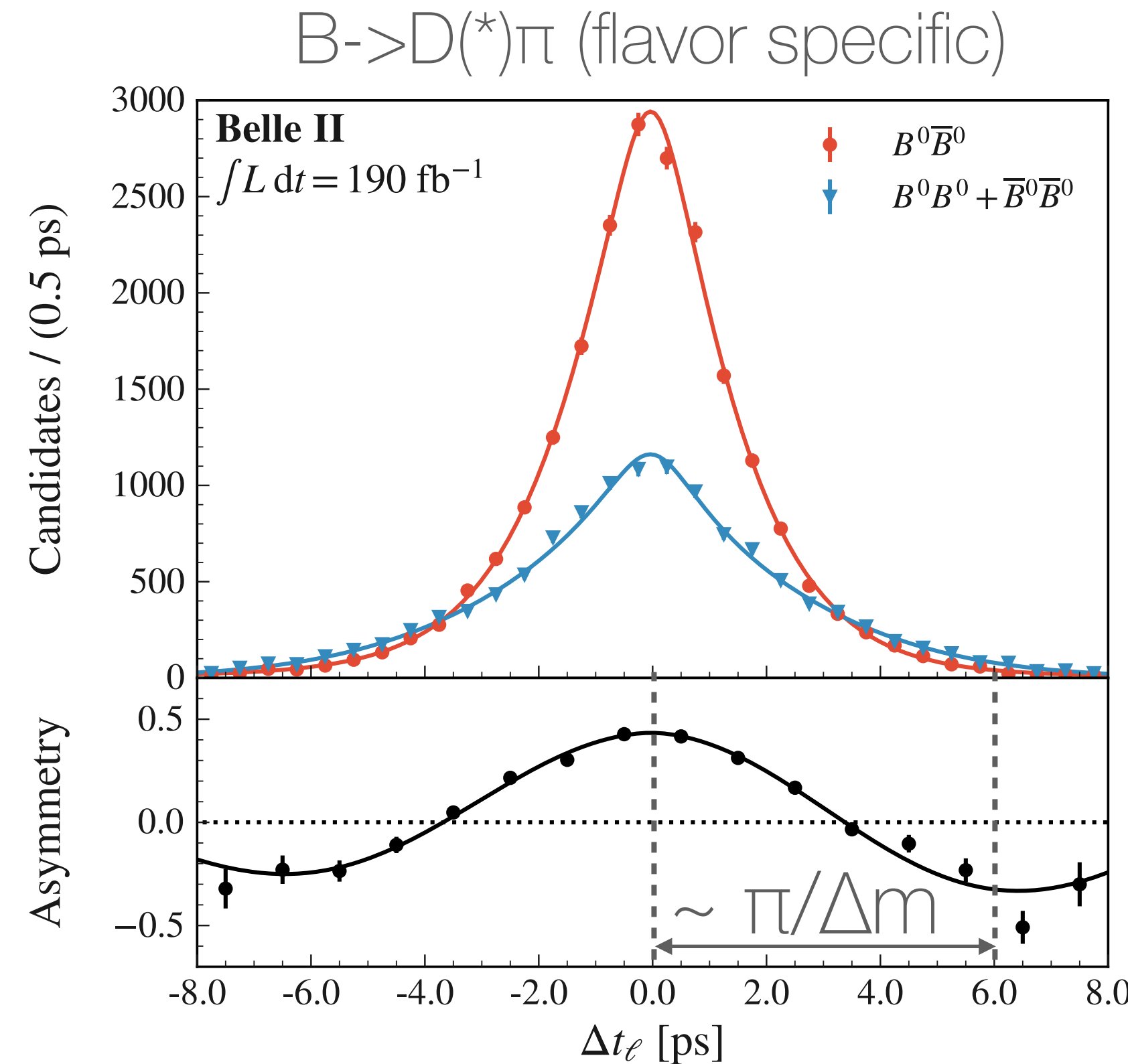
Pixel detector radius  $\approx 1.4$  cm

# $\Delta m$ and $\sin 2\phi_1$



- High-yield, low-background modes used for benchmark measurements of time-dependent observables
- Main challenge: accurate understanding of vertex resolution ( $\Delta t$  resolution  $\sim 1$  ps) and tagging ( $\epsilon_{\text{tag}} \sim 30\%$ )

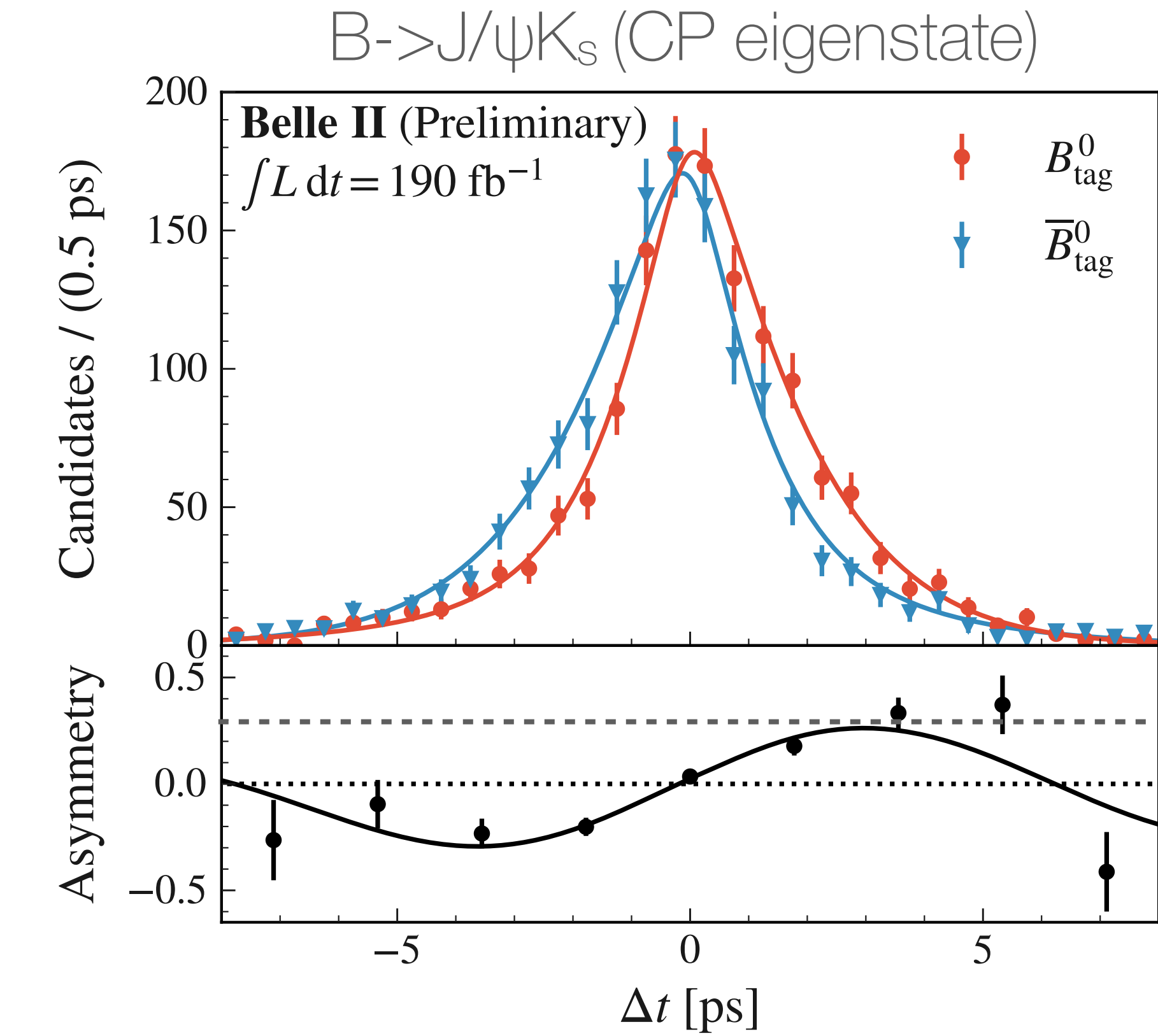
# $\Delta m$ and $\sin 2\phi_1$



$$\tau_{B^0} = (1.499 \pm 0.013 \pm 0.008) \text{ ps}$$

$$\Delta m_d = (0.516 \pm 0.008 \pm 0.005) \text{ ps}^{-1}$$

HFLAV:  $\tau = 1.519 \pm 0.004$  ps,  
 $\Delta m = 0.5065 \pm 0.0019 \text{ ps}^{-1}$



$$S_{CP} = 0.720 \pm 0.062(\text{stat}) \pm 0.016(\text{syst})$$

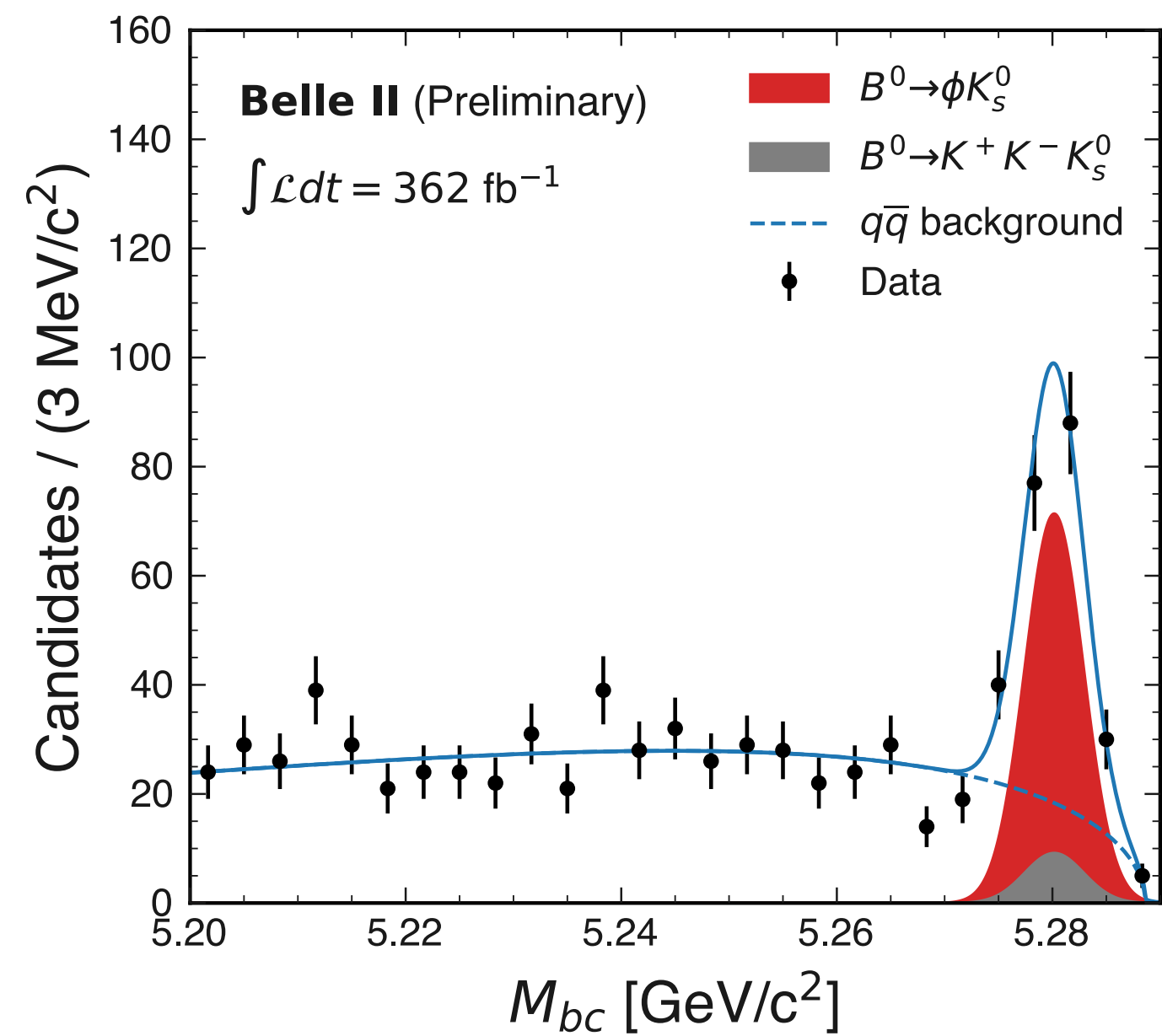
$$A_{CP} = 0.094 \pm 0.044(\text{stat}) \pm 0.017(\text{syst})$$

HFLAV:  $S = 0.699 \pm 0.017$ ,  
 $A = 0.005 \pm 0.015$

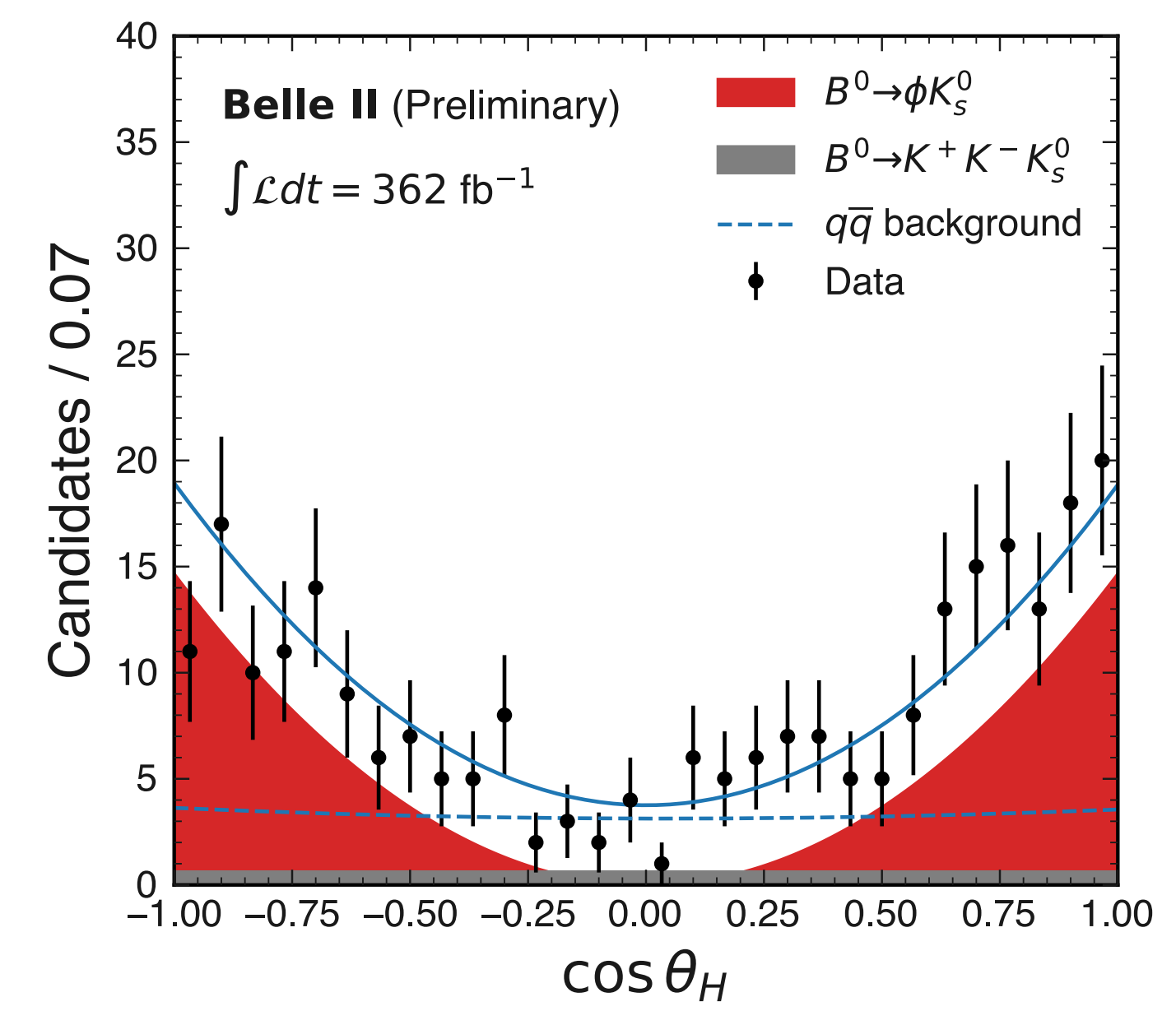
# $B \rightarrow \phi K_s$ NEW FOR MORIOND

- Clean experimental signature with similar  $\Delta t$  resolution as  $B \rightarrow J/\psi K_s$
- Main challenge: dilution from non-resonant decays with opposite CP
- Quasi-two body analysis of resonant  $B \rightarrow \phi K_s$  decays
  - ▶ Non-resonant  $B \rightarrow K^+ K^- K_s^0$  component disentangled in  $\cos\theta$
  - ▶ Effect of neglecting interference estimated with inputs from previous Dalitz measurements

Beam-constrained mass



Cosine of the helicity angle

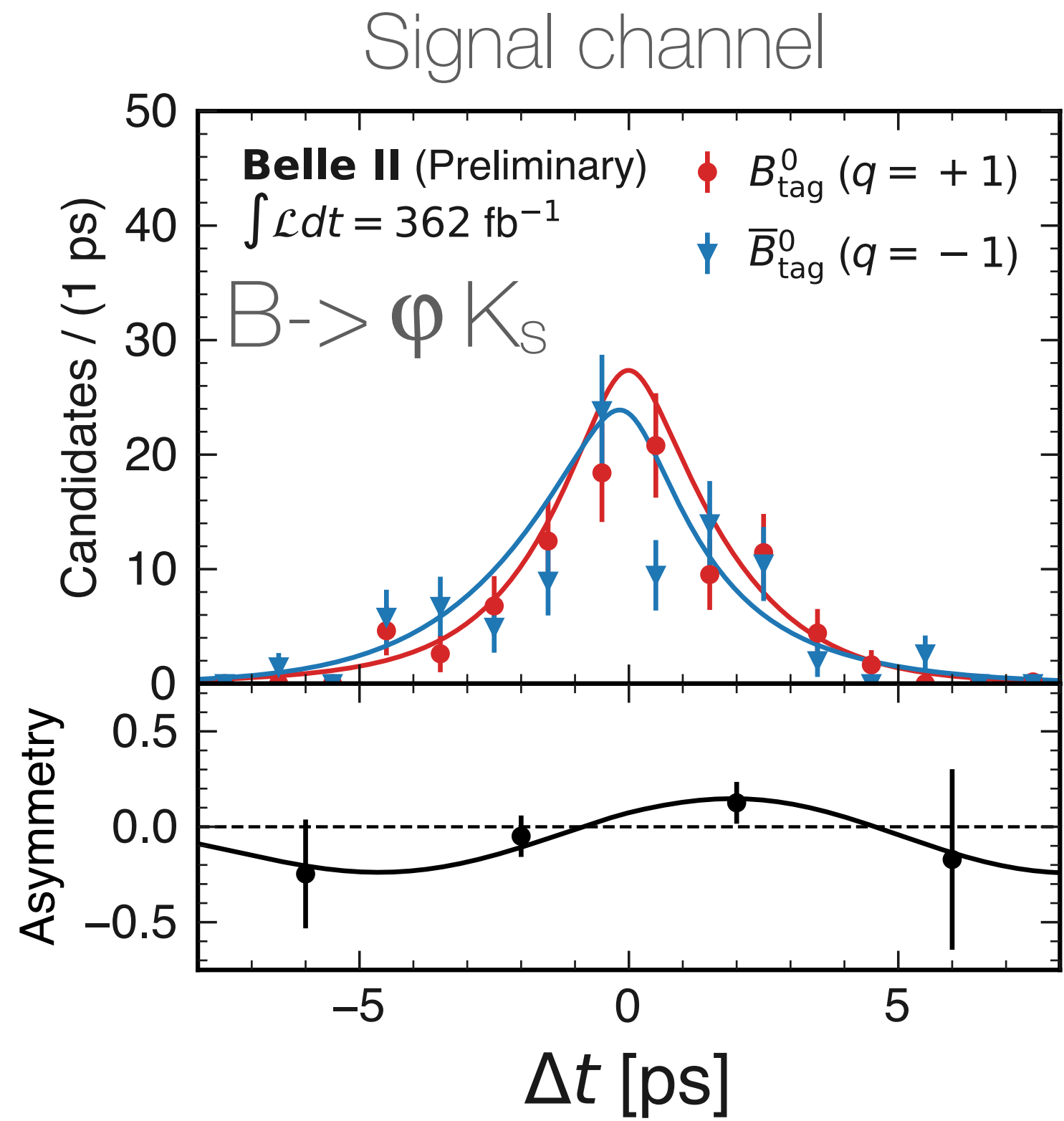


$162 \pm 17$   $B \rightarrow \phi K_s$  signal events with 387M  $B\bar{B}$  pairs

# $B \rightarrow \phi K_s$ NEW FOR MORIOND

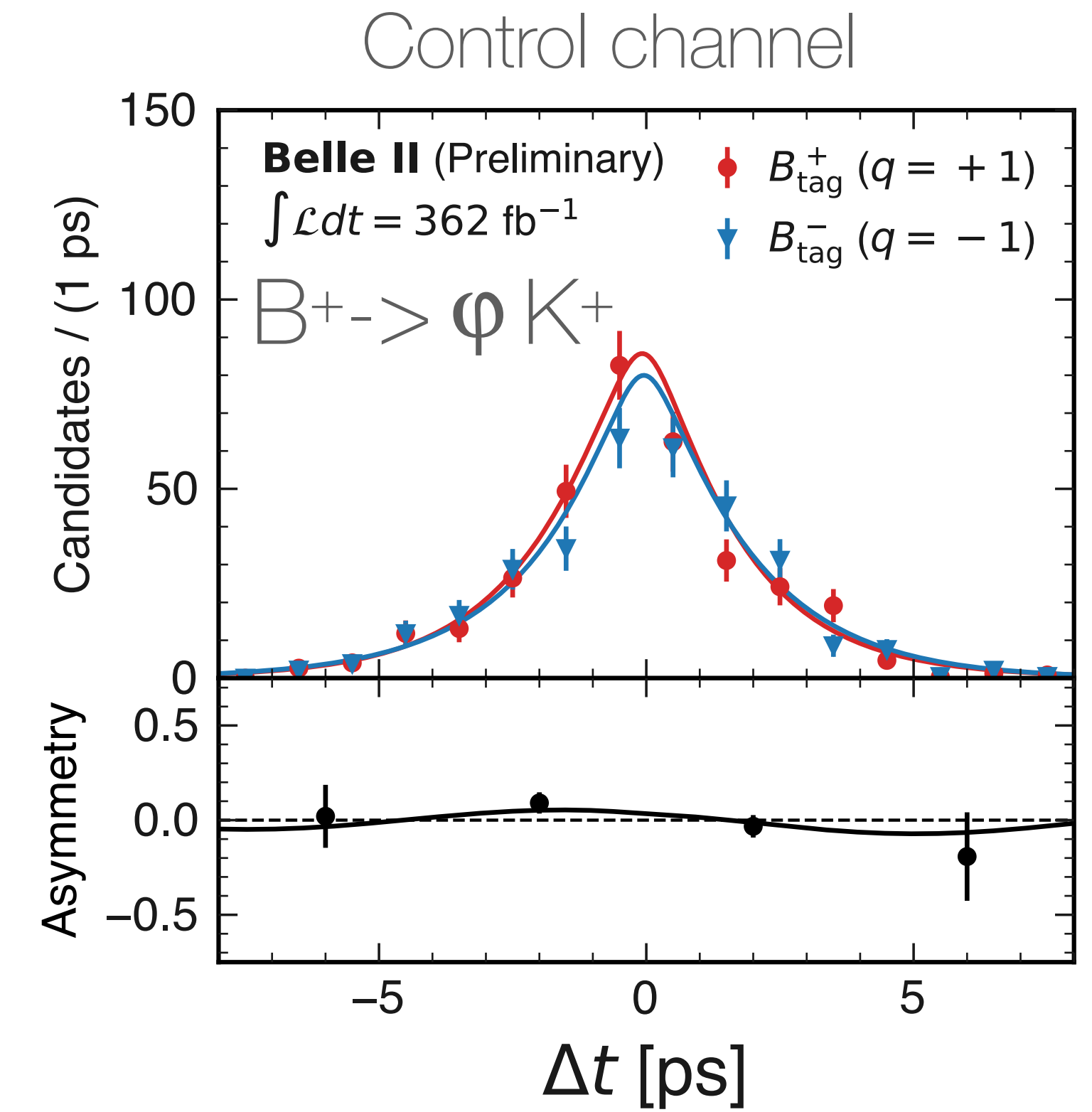
(background subtracted)

- Simultaneous  $\Delta t$  fit to extract the CP asymmetries
  - ▶  $B \rightarrow K^+ K^- K_s$  fixed from HFLAV
  - ▶ Validated on the  $B^+$  control sample (null asymmetry)
- Mostly unique to Belle II
  - ▶ On par with most precise determinations of  $A_{CP}$
  - ▶ 10-20% improvement on  $S_{CP}$  for the same signal yield wrt Belle/BaBar determinations



$$A_{CP} = 0.31 \pm 0.20^{+0.05}_{-0.06}$$

$$S_{CP} = 0.54 \pm 0.26^{+0.06}_{-0.08}$$



$$A_{CP} = 0.12 \pm 0.10 \text{ (stat.)}$$

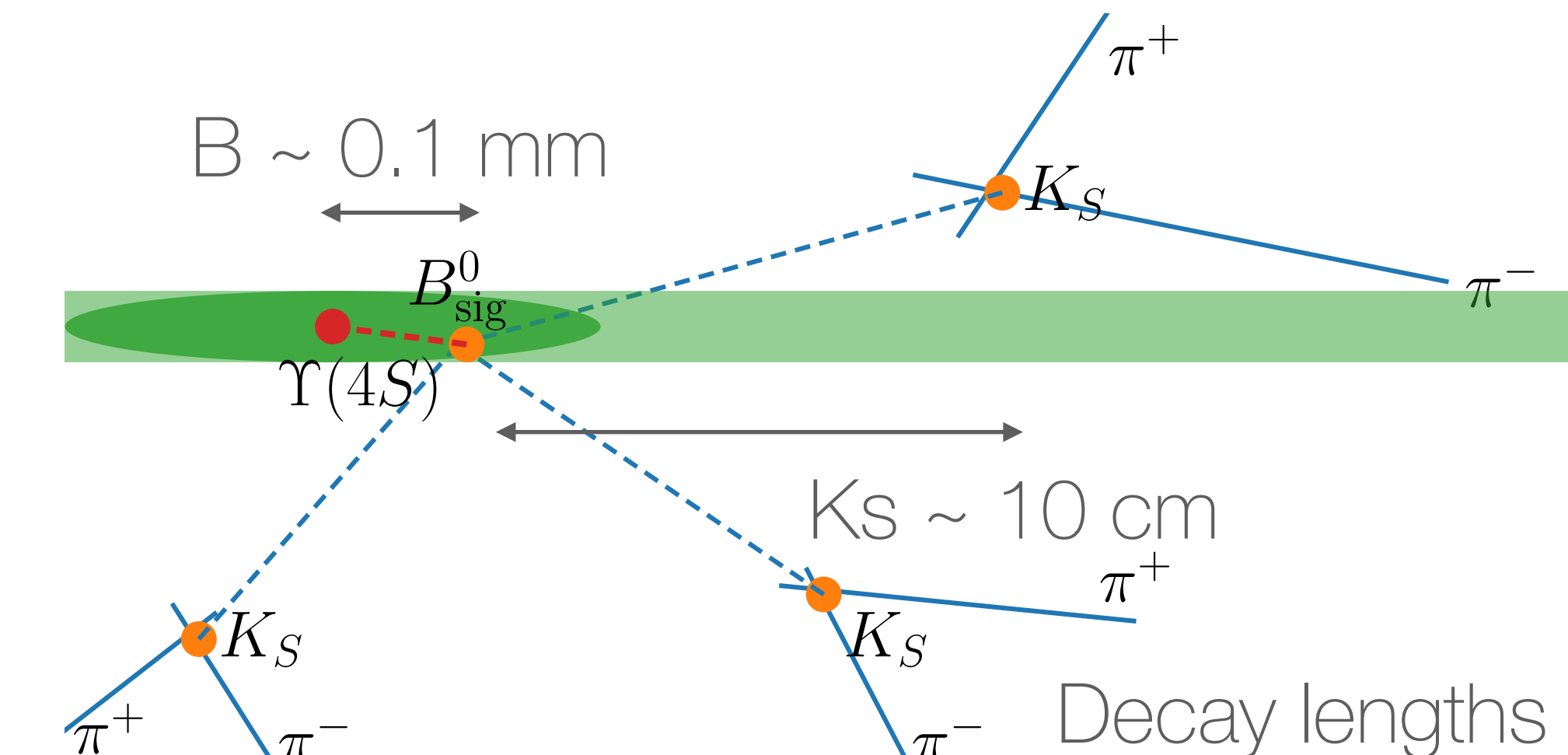
$$S_{CP} = -0.09 \pm 0.12 \text{ (stat.)}$$

HFLAV:  $S = 0.74^{+0.11}_{-0.13}$ ,  $A = -0.01 \pm 0.14$

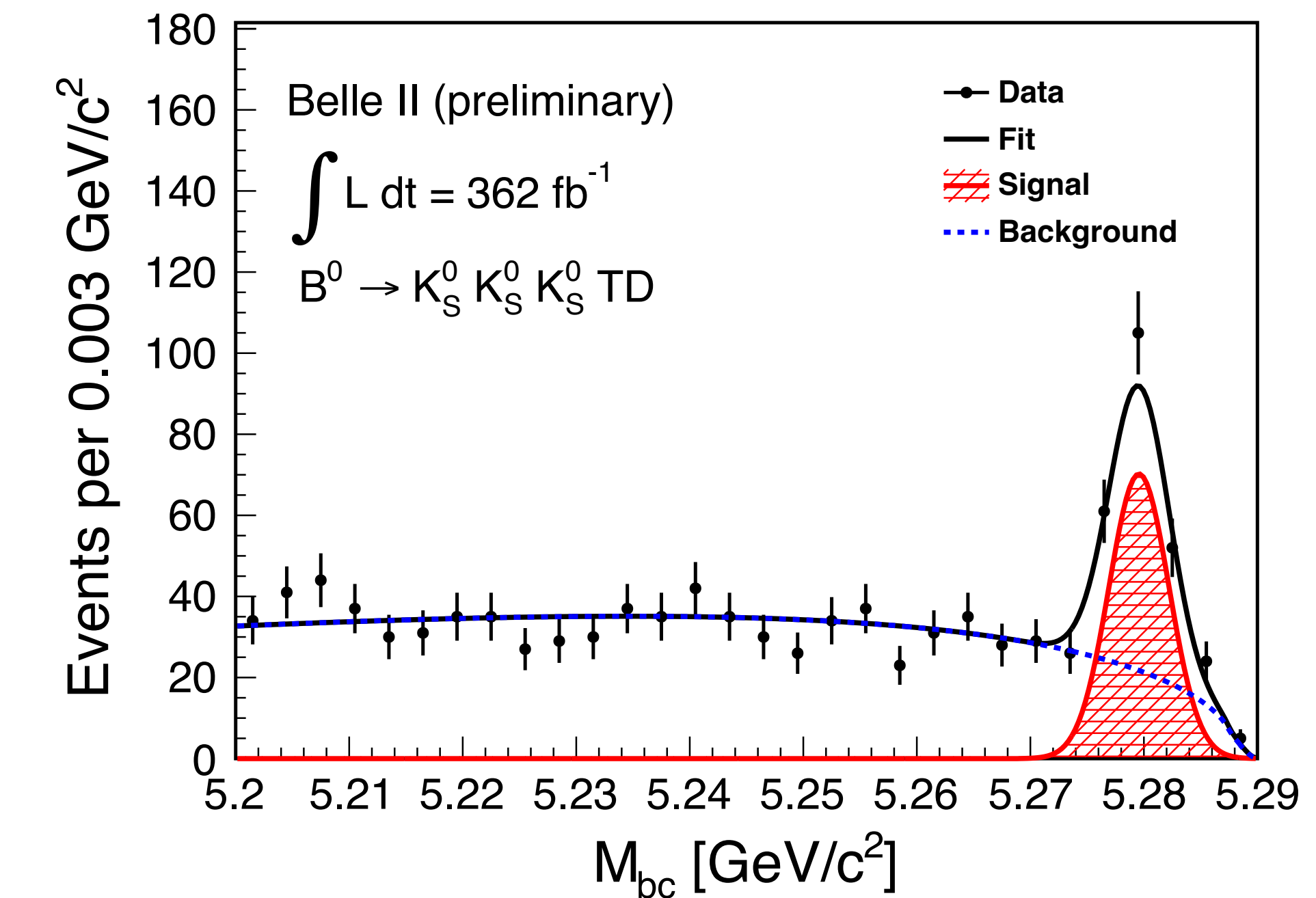
# $B \rightarrow K_s K_s K_s$ NEW FOR MORIOND

- Same underlying quark transition as  $B \rightarrow \varphi K_s$ , w/o contributions from opposite-CP backgrounds
- Main challenge: no prompt tracks to form a vertex
  - ▶ Decay vertex reconstruction relies on the  $K_s$  trajectory and profile of the interaction point
  - ▶ Dataset divided into events with (TD) and without (TI) information from the vertex detector
- 2 BDTs to suppress fake  $K_s$  (kinematic/hits  $\pi^\pm$  tracks) and continuum (event shape variables)

$158^{+14}_{-13}$  (TD) +  $62 \pm 9$  (TI)  $B \rightarrow K_s K_s K_s$   
signal events with 387M  $B\bar{B}$  pairs



Beam-constrained mass



# $B \rightarrow K_s K_s K_s$ NEW FOR MORIOND

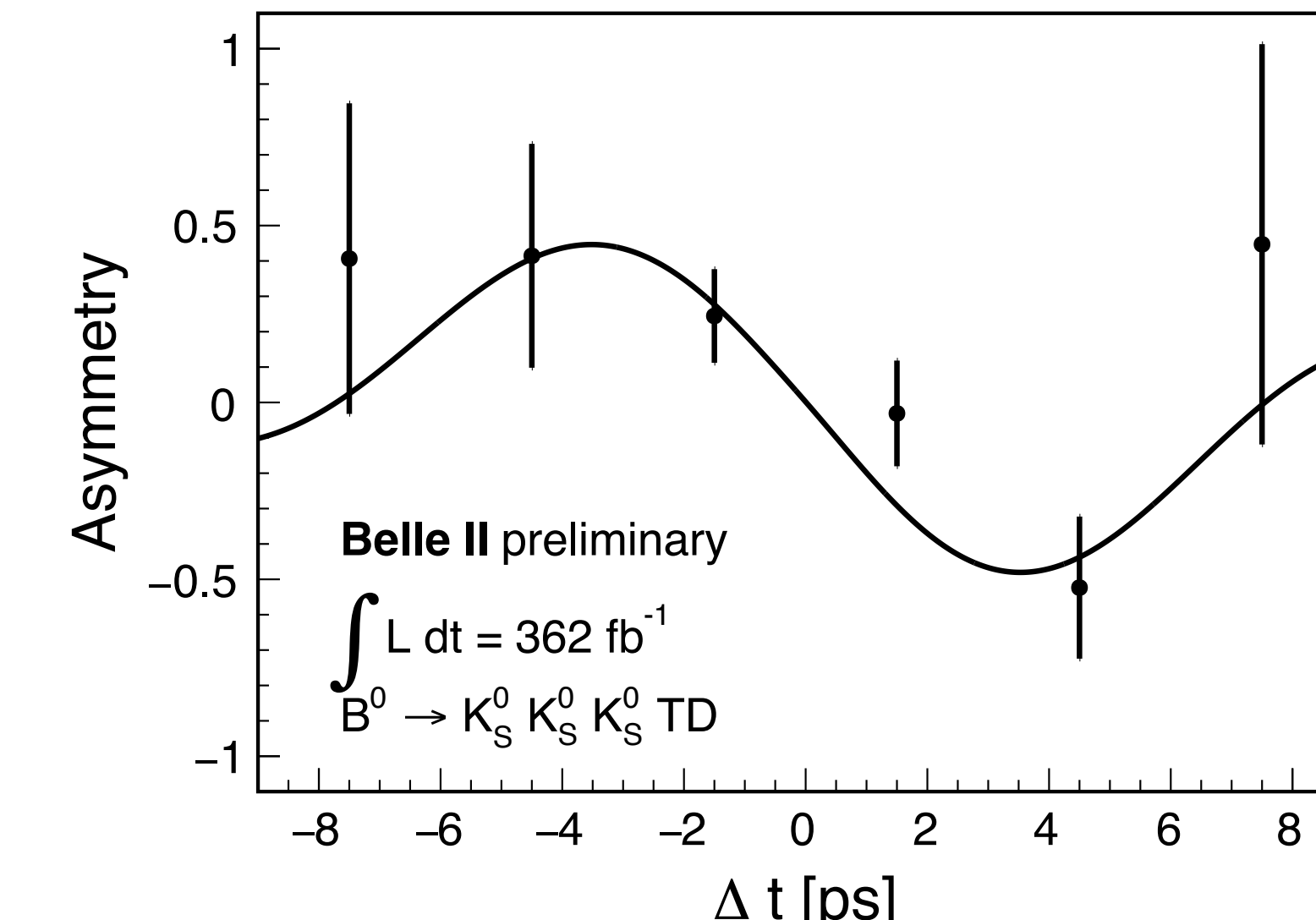
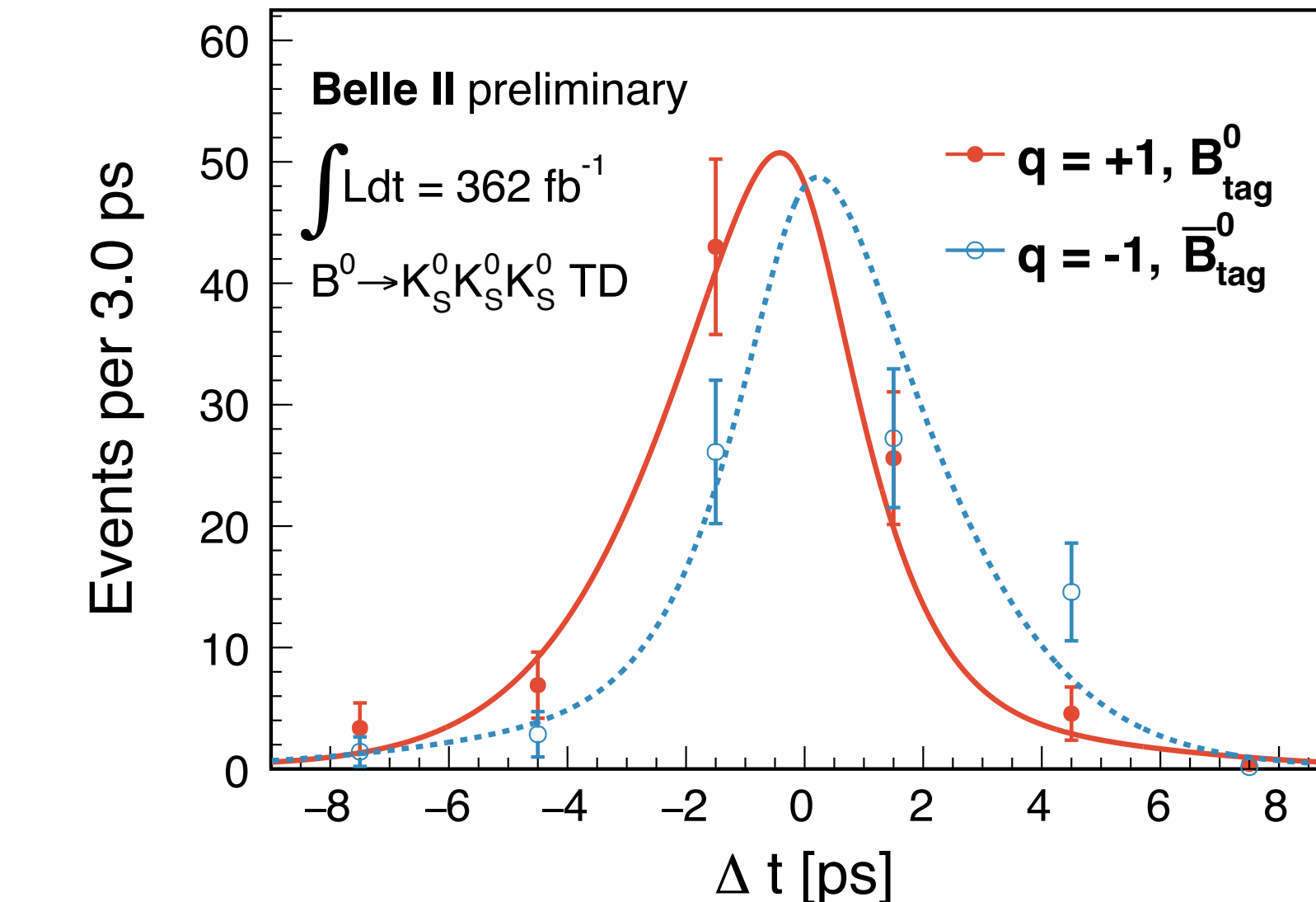
(background subtracted)

- Simultaneous fit to TI, TD events and  $B^+ \rightarrow K_s K_s K^+$ 
  - ▶ TD events used in the  $\Delta t$  fit for the determination of  $A_{CP}$  and  $S_{CP}$
  - ▶ TI events used only to constrain the time-integrated asymmetry  $A_{CP}$
  - ▶  $B^+ \rightarrow K_s K_s K^+$  control sample to constrain background shapes and  $\Delta t$  resolution function
- On par with most precise determination of  $A_{CP}$  and unique to Belle II

$$A_{CP} = 0.07^{+0.15}_{-0.20} \pm 0.02$$

$$S_{CP} = -1.37^{+0.35}_{-0.45} \pm 0.03$$

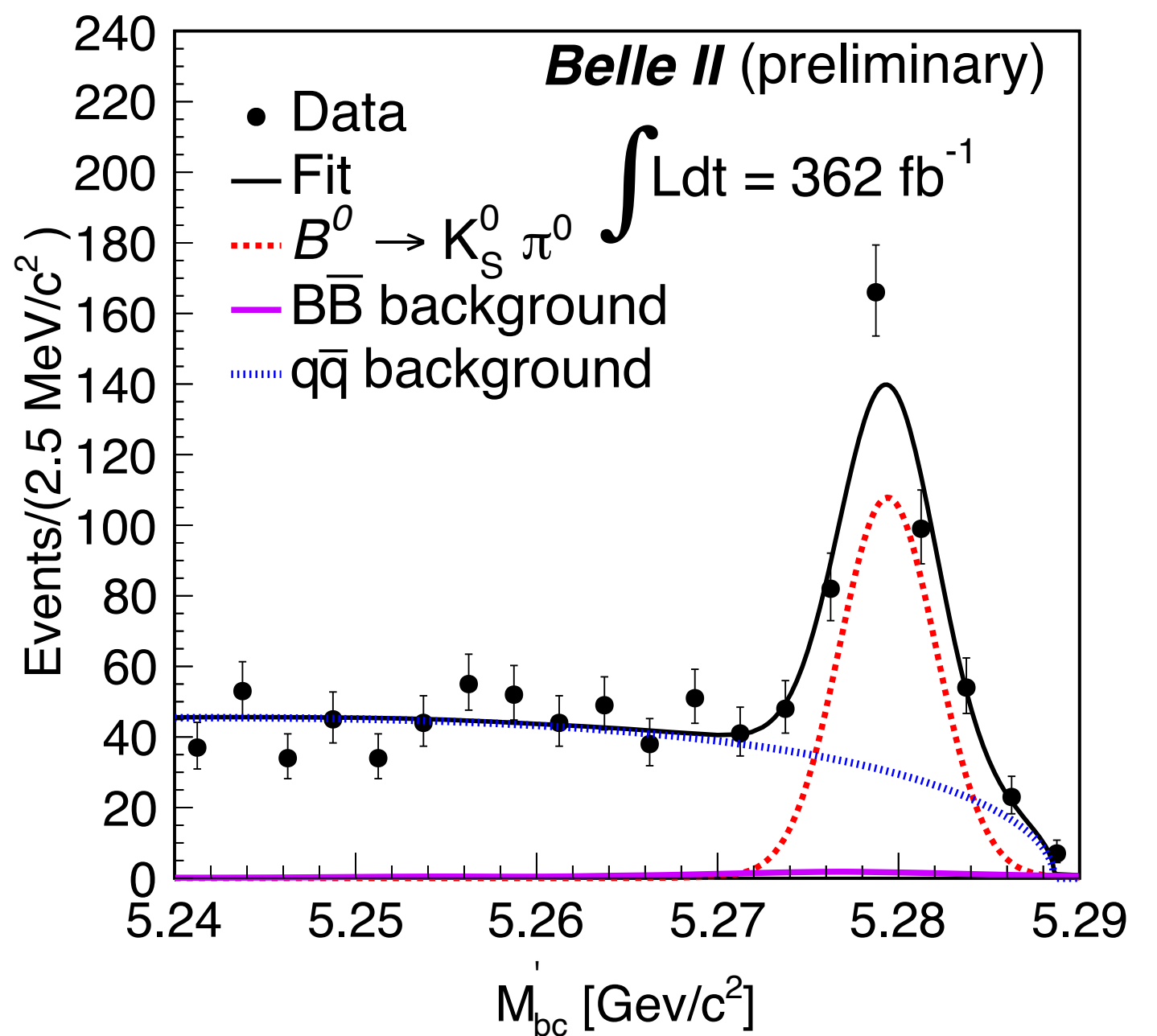
HFLAV:  $S = -0.83 \pm 0.17$ ,  $A = 0.15 \pm 0.12$



# $B \rightarrow K_s \pi^0$ NEW FOR MORIOND

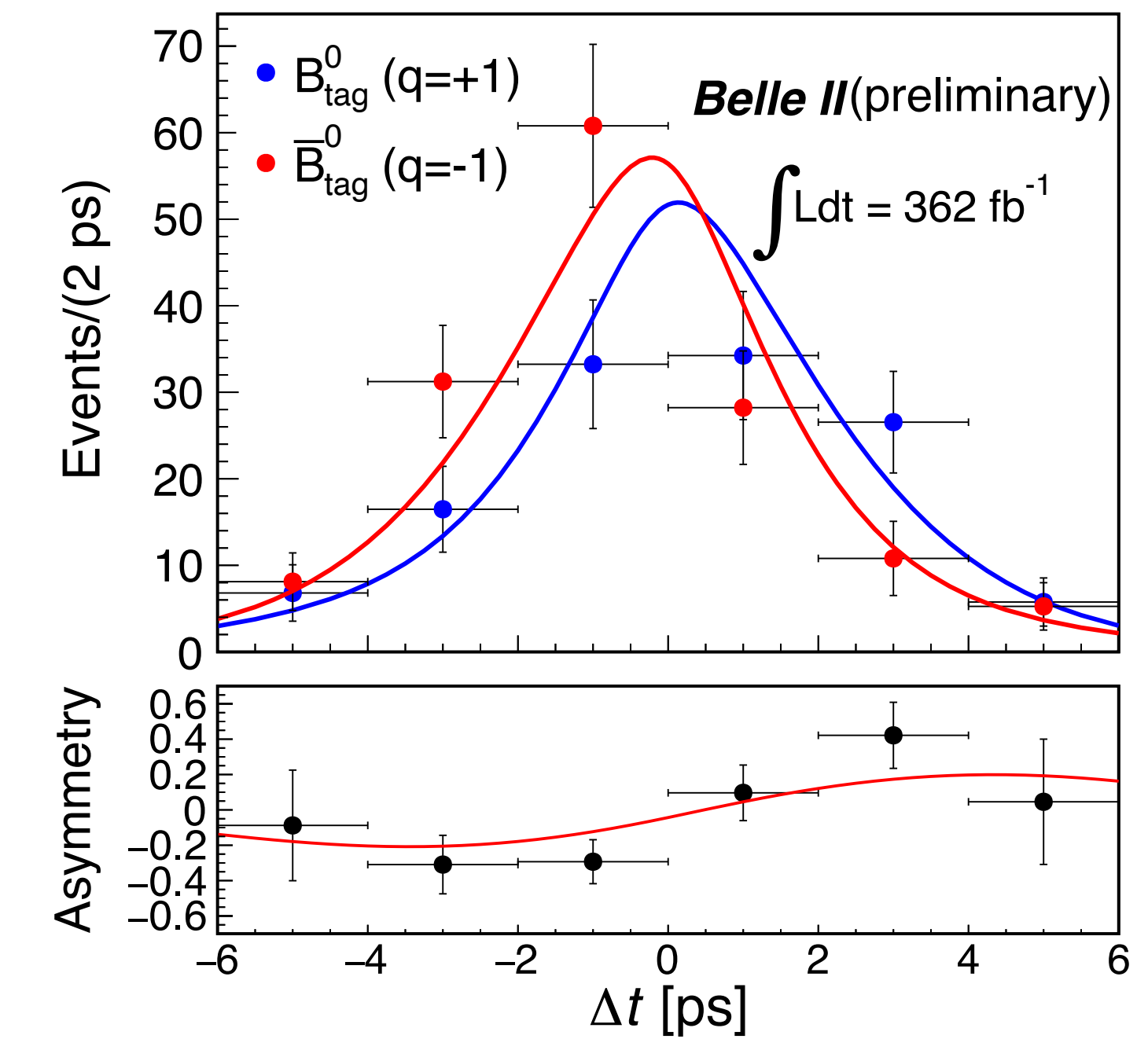
- Sensitive to effective value of  $\sin 2\phi_1$  and providing inputs to isospin sum-rule
  - See Sagar's talk this afternoon
- Needs excellent capabilities with neutrals, unique to Belle II
  - Validated on  $B \rightarrow J/\psi K_s$  events reconstructed w/o  $J/\psi$  vertex
  - Simultaneous TI/TD fit to maximize the sensitivity on  $A_{CP}$
- Competitive with world's best results with much less luminosity

Beam-constrained mass



$415^{+26}_{-25}$   $B \rightarrow K_s \pi^0$   
signal events with  
387M  $BB$  pairs

(background subtracted)



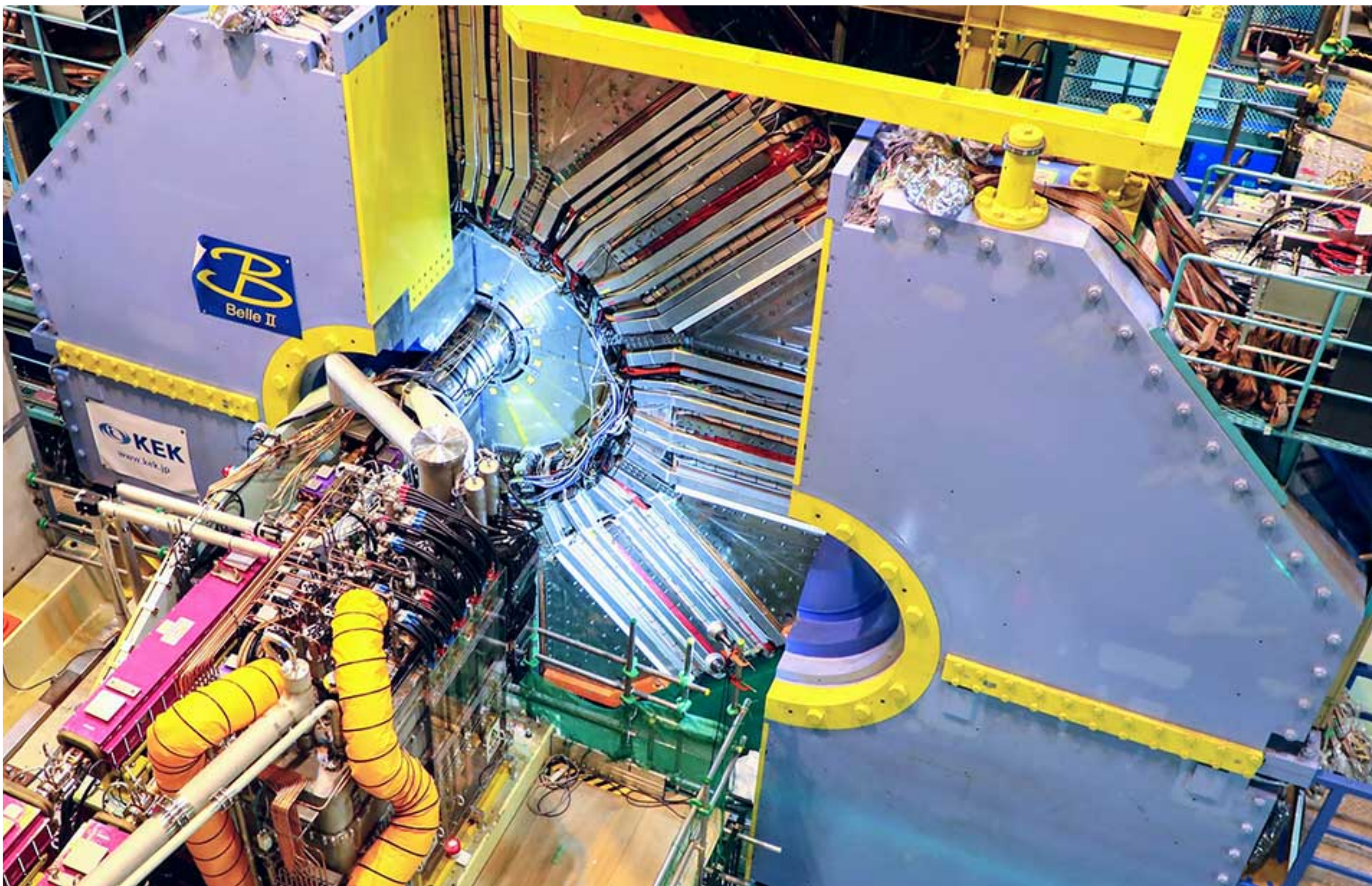
$$A_{CP} = 0.04 \pm 0.15 \pm 0.05$$

$$S_{CP} = 0.75^{+0.20}_{-0.23} \pm 0.04$$

HFLAV:  $S = 0.57 \pm 0.17$ ,  $A = -0.01 \pm 0.10$

# Summary

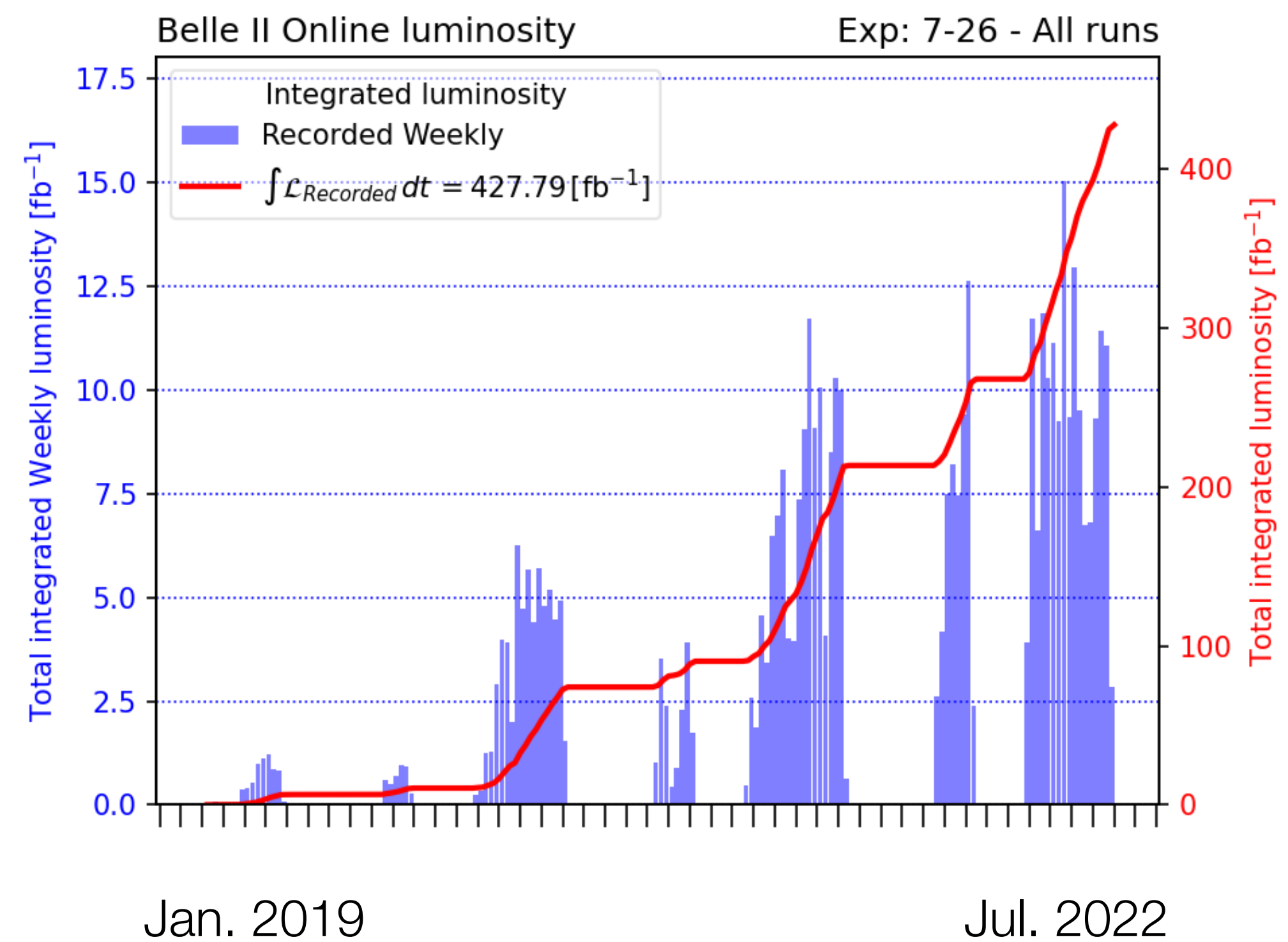
- **3 new results** on time-dependent CP observables with penguins for Moriond
  - ▶ Precision on par with world's best determinations in spite of much less luminosity
- These measurements are essential to probe generic BSM physics in loops
  - ▶ Belle II is in a unique position to improve our current experimental knowledge on these modes



# Backup

# Collected luminosity

- Collected  $424 \text{ fb}^{-1}$  in 2019-2022
  - $362 \text{ fb}^{-1}$  at 4S ( $387 \times 10^6 B\bar{B}$  pairs)
  - $42.3 \text{ fb}^{-1}$  at 4S off-resonance
  - $78 \text{ pb}^{-1}$  at 4S scan
  - $19.7 \text{ fb}^{-1}$  at energy scan



# Long-shutdown activity and plans

---

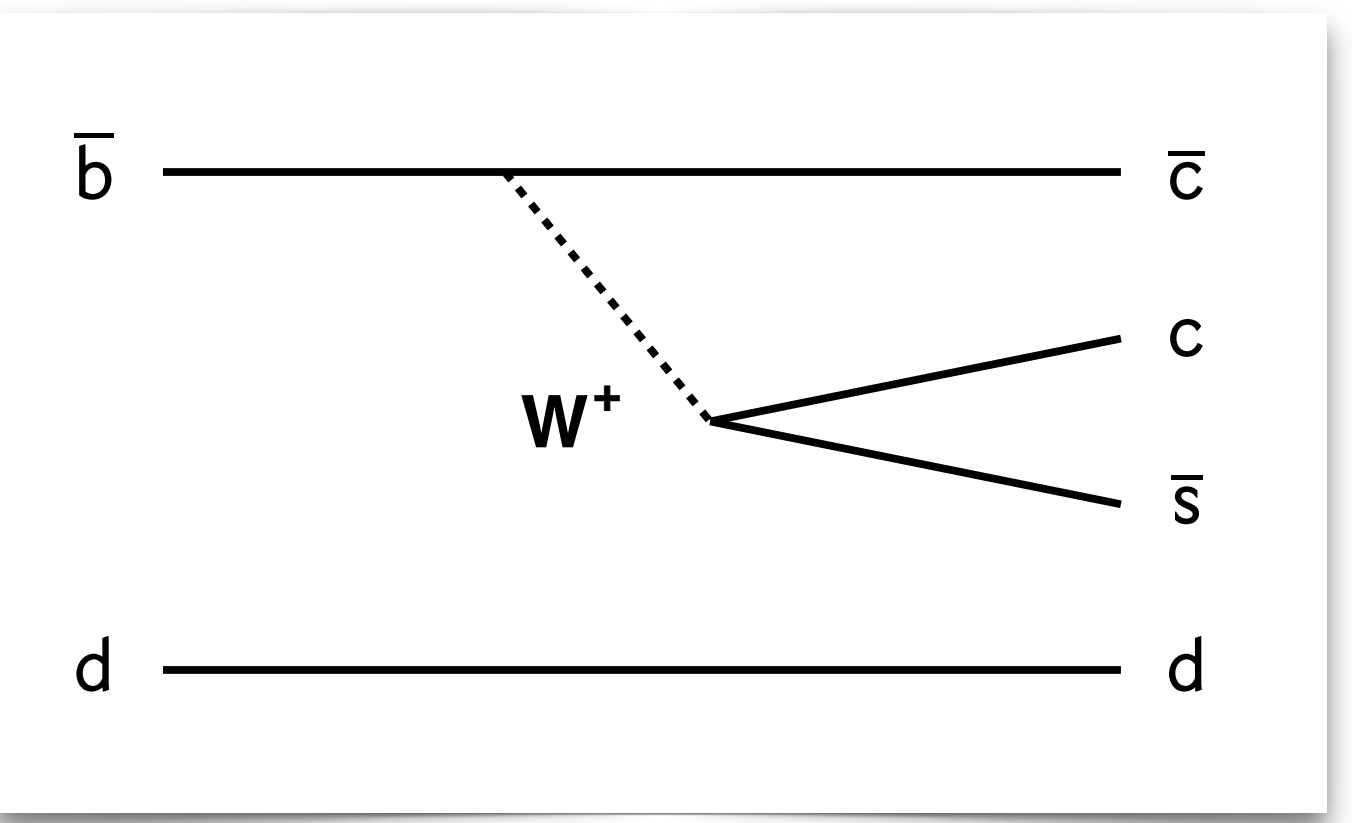
Belle II stopped taking data in Summer 2022 for a long shutdown for

- replacement of beam-pipe
- replacement of photomultipliers of the central PID detector (TOP)
- installation of 2-layered pixel vertex detector
- improved data-quality monitoring and alarm system
- complete transition to new DAQ boards (PCIe40)
- replacing of ageing components
- additional shielding and increased resilience against beam background

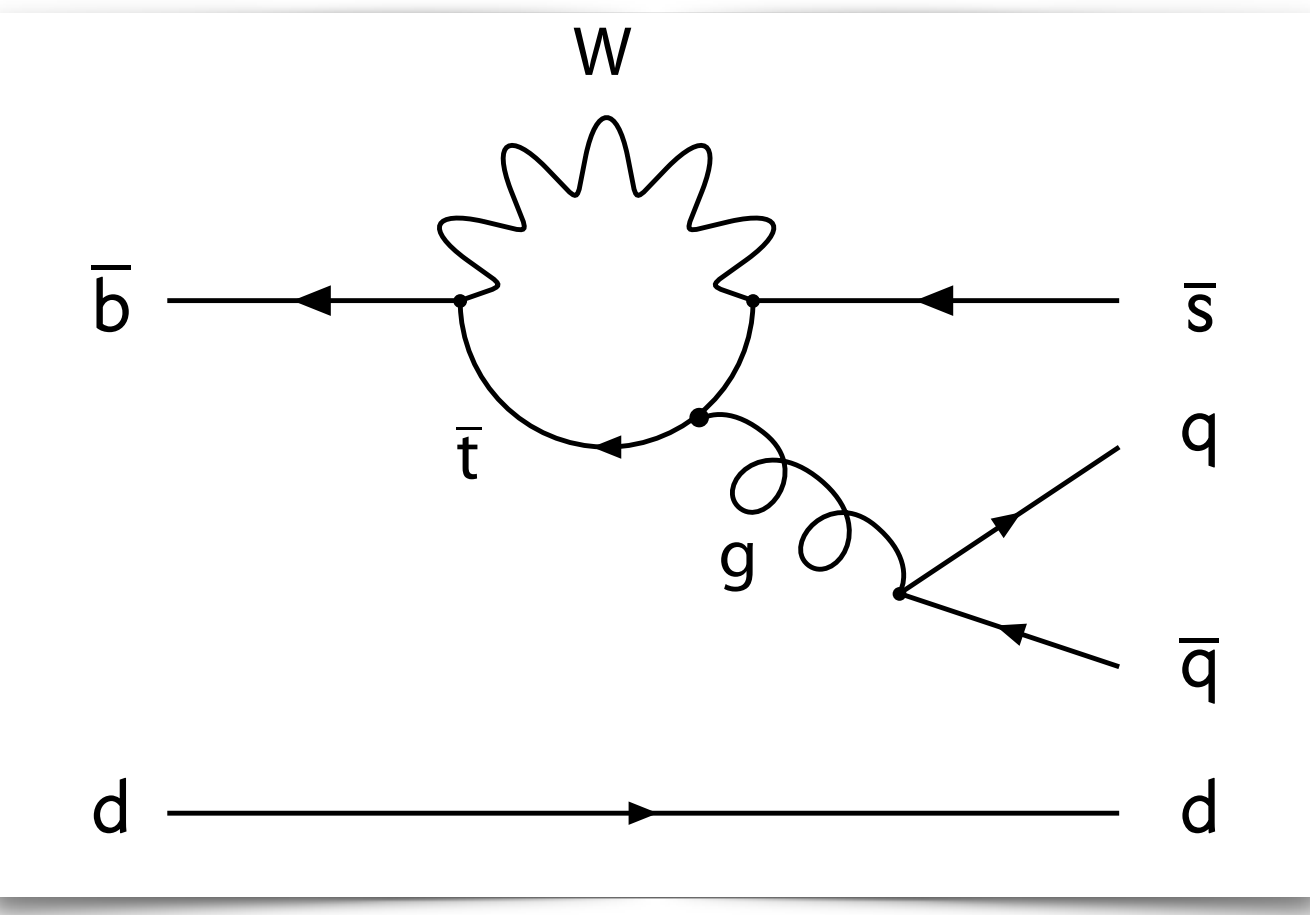
Currently working on pixel detector installation:

- shipping to KEK in mid March
- final test in KEK scheduled in April

On track to resume data taking next Winter with new pixel detector.



“Tree”  $b \rightarrow c\bar{c}s$   
e.g.  $B \rightarrow J/\psi K_s$



“Penguin”  $b \rightarrow q\bar{q}s$   
e.g.  $B \rightarrow \varphi K_s$ ,  $B \rightarrow K_s \pi^0$ ,  
 $B \rightarrow K_s K_s K_s$

# $b \rightarrow c\bar{c}s$

Experiment	Sample size	$-\eta S_{b \rightarrow c\bar{c}s}$	$C_{b \rightarrow c\bar{c}s}$
Most precise			
<i>BABAR</i> $b \rightarrow c\bar{c}s$	[324]	$N(B\bar{B}) = 465M$	$0.687 \pm 0.028 \pm 0.012$
<i>Belle</i> $b \rightarrow c\bar{c}s$	[325]	$N(B\bar{B}) = 772M$	$0.667 \pm 0.023 \pm 0.012$
LHCb $J/\psi K_s^0$	[326, 327]	$\int \mathcal{L} dt = 3 \text{ fb}^{-1}$	$0.75 \pm 0.04$
LHCb $\psi(2S)K_s^0$	[327]	$\int \mathcal{L} dt = 3 \text{ fb}^{-1}$	$0.84 \pm 0.10 \pm 0.01$
<i>Belle II</i> (200M BB pairs) <a href="https://arxiv.org/abs/2302.12898">[arXiv:2302.12898]</a>		<b><math>0.720 \pm 0.062 \pm 0.016</math></b>	<b><math>-0.094 \pm 0.044^{+0.042}_{-0.017}</math></b>

# $b \rightarrow q\bar{q}s$

Experiment		$N(B\bar{B})$	$-\eta S_{b \rightarrow q\bar{q}s}$	$C_{b \rightarrow q\bar{q}s}$
			$\phi K^0$	
<i>BABAR</i>	[262]	470M	$0.66 \pm 0.17 \pm 0.07$	$0.05 \pm 0.18 \pm 0.05$
Belle	[261]	657M	$0.90^{+0.09}_{-0.19}$	$-0.04 \pm 0.20 \pm 0.10 \pm 0.02$
Belle II (362M BB pairs)			$0.54 \pm 0.26^{+0.06}_{-0.08}$	$-0.31 \pm 0.20^{+0.05}_{-0.06}$
			$K_s^0 K_s^0 K_s^0$	
<i>BABAR</i>	[383]	468M	$0.94^{+0.21}_{-0.24} \pm 0.06$	$-0.17 \pm 0.18 \pm 0.04$
Belle	[384]	722M	$0.71 \pm 0.23 \pm 0.05$	$-0.12 \pm 0.16 \pm 0.05$
Belle II (362M BB pairs)			$-1.37^{+0.35}_{-0.45} \pm 0.03$	$-0.07^{+0.15}_{-0.20} \pm 0.02$
			$\pi^0 K^0$	
<i>BABAR</i>	[381]	467M	$0.55 \pm 0.20 \pm 0.03$	$0.13 \pm 0.13 \pm 0.03$
Belle	[378]	657M	$0.67 \pm 0.31 \pm 0.08$	$-0.14 \pm 0.13 \pm 0.06$
Belle II (362M BB pairs)			$0.74^{+0.20}_{-0.23} \pm 0.04$	$-0.04 \pm 0.15 \pm 0.05$

# Systematic uncertainties (1)

$B \rightarrow D^{(*)}\pi$

TABLE I. Systematic uncertainties.

Source	$\tau_{B^0}$ [ps]	$\Delta m_d$ [ps $^{-1}$ ]
Fixed response-function parameters	0.006	0.003
Analysis bias	0.004	0.001
Detector alignment	0.003	0.002
Interaction-region precision	0.002	0.001
$C$ -Distribution modeling	0.000	0.001
$\sigma_{\Delta t_\ell}$ -Distribution modeling	0.001	0.001
Correlations of $\Delta E$ or $C$ and $\Delta t_\ell$	0.001	0.000
Total systematic uncertainty	0.008	0.005
Statistical uncertainty	0.013	0.008

$B \rightarrow J/\psi K_s$

TABLE II. Summary of the individual sources of uncertainties.

Source	$\sigma(S_{CP})$	$\sigma(A_{CP})$
Statistical	0.0622	0.0439
Calibration with $B^0 \rightarrow D^{(*)-}\pi^+$ decays		
$B^0 \rightarrow D^{(*)-}\pi^+$ sample size	0.0111	0.0093
Signal charge-asymmetry	0.0027	0.0126
$w_6^+ = 0$ limit	0.0014	0.0001
Fit model		
Analysis bias	0.0080	0.0020
Fixed resolution parameters	0.0039	0.0008
$\sigma_{\Delta t}$ binning	0.0050	0.0051
$\tau_{B^0}, \Delta m_d$	0.0007	0.0002
$\Delta t$ measurement		
Alignment	0.0020	0.0042
Beam spot	0.0024	0.0020
Momentum scale	0.0005	0.0013
$B^0 \rightarrow J/\psi K_S^0$ $\Delta E$ background shape	0.0037	0.0015
Multiple candidates	0.0005	0.0008
$CP$ violation in $B_{tag}^0$ decays	0.0020	$^{+0.0380}_{-0.0000}$
Total systematic	0.0163	$^{+0.0418}_{-0.0174}$

# Systematic uncertainties (2)

$B \rightarrow K_S \pi^0$

Source	$\delta A_{CP}$	$\delta S_{CP}$
Flavor tagging	0.013	0.011
Resolution function	0.014	0.022
$B\bar{B}$ background asymmetry	0.030	0.018
$q\bar{q}$ background asymmetry	0.028	< 0.001
Signal modelling	0.004	0.003
Background modelling	0.006	0.018
Possible fit bias	0.005	0.011
External inputs	< 0.001	< 0.001
Tag-side interference	0.008	0.010
VXD misalignment	0.004	0.005
<b>Total</b>	<b>0.045</b>	<b>0.039</b>

$B \rightarrow K_S K_S K_S$

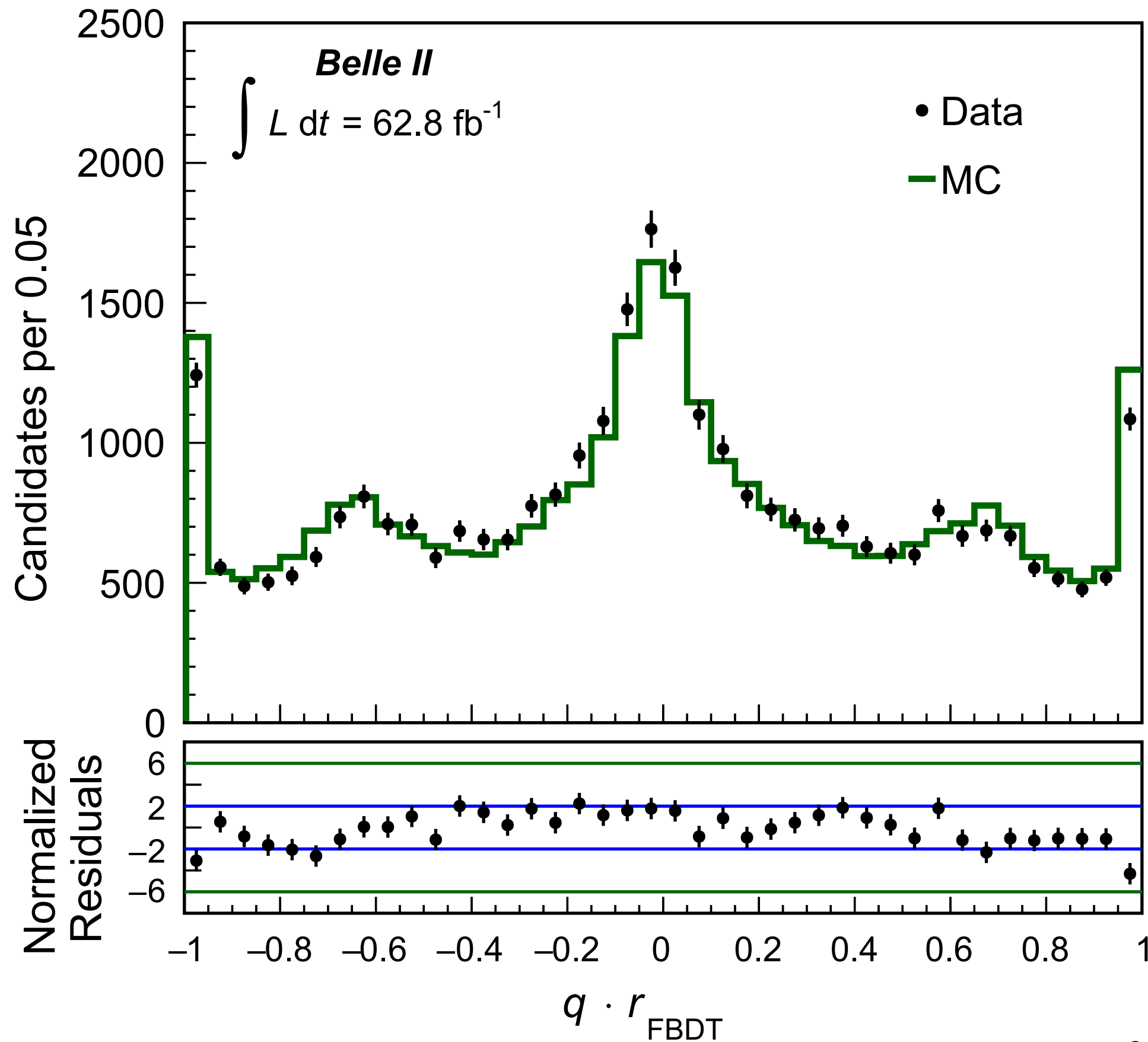
Source	$\delta S$	$\delta A$
Signal probability	0.014	0.008
Fit bias	0.014	0.004
Flavor tagging	0.013	0.012
Resolution function	0.013	0.008
Tag-side interference	0.011	0.006
Vertex reconstruction	0.011	0.004
Physics parameters	0.009	0.000
Detector misalignment	0.008	0.007
Background $\Delta t$ shape	0.004	0.002
<b>Total</b>	<b>0.032</b>	<b>0.020</b>

$B \rightarrow \phi K_S$

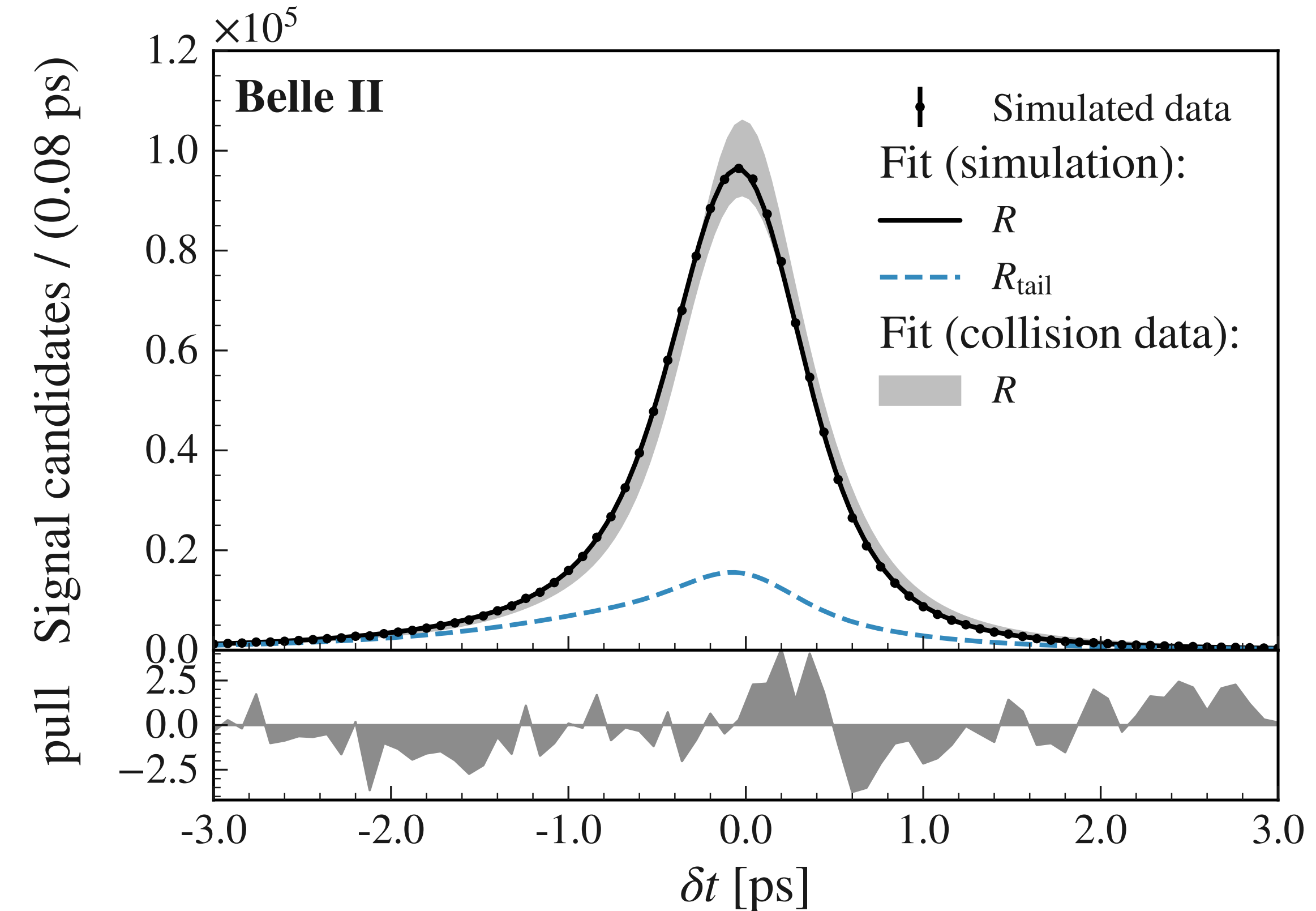
Source	$\sigma(A_{CP})$	$\sigma(S_{CP})$
Calibration with $B^0 \rightarrow D^{(*)-} \pi^+$ decays		
Calibration sample size	0.010	0.009
Calibration sample systematic	0.010	0.012
Portability to $B^0 \rightarrow \phi K_S^0$	+0.000 -0.005	+0.021 -0.000
Analysis model		
Fit bias	+0.017 -0.028	+0.033 -0.062
Correlations between observables	+0.000 -0.030	+0.002 -0.000
$B^0 \rightarrow K^+ K^- K_S^0$ backgrounds	+0.000 -0.020	+0.000 -0.011
Fixed fit shapes	0.009	0.022
$\tau_d$ and $\Delta m_d$	0.006	0.022
$A_{CP}^{K^+ K^- K}$ and $S_{CP}^{K^+ K^- K}$	0.014 +0.030	0.013 +0.017
$B\bar{B}$ backgrounds	-0.019 +0.000	-0.031 +0.012
Tag-side interference	-0.000 +0.032	-0.000 +0.000
Multiple candidates	+0.032 -0.000	+0.000 -0.003
$\Delta t$ measurement		
Detector misalignment	+0.002 -0.000	+0.000 -0.002
Momentum scale	0.001	0.001
Beam spot	0.002	0.002
$\Delta t$ approximation	+0.000 -0.000	+0.000 -0.018
<b>Total systematic</b>	<b>+0.052 -0.055</b>	<b>+0.058 -0.082</b>
<b>Statistical</b>	<b>0.201</b>	<b>0.256</b>

# Flavor tagging and resolution

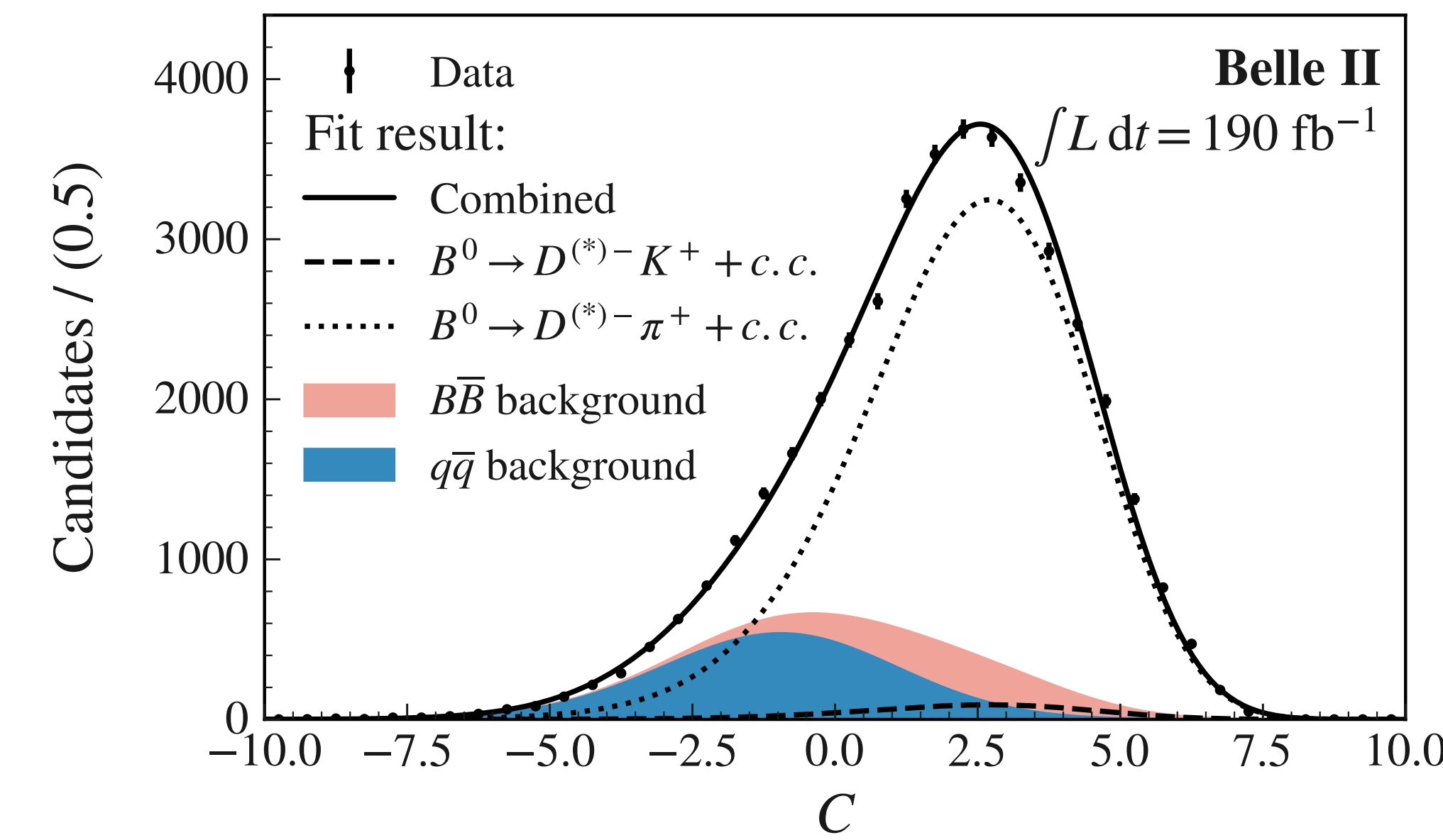
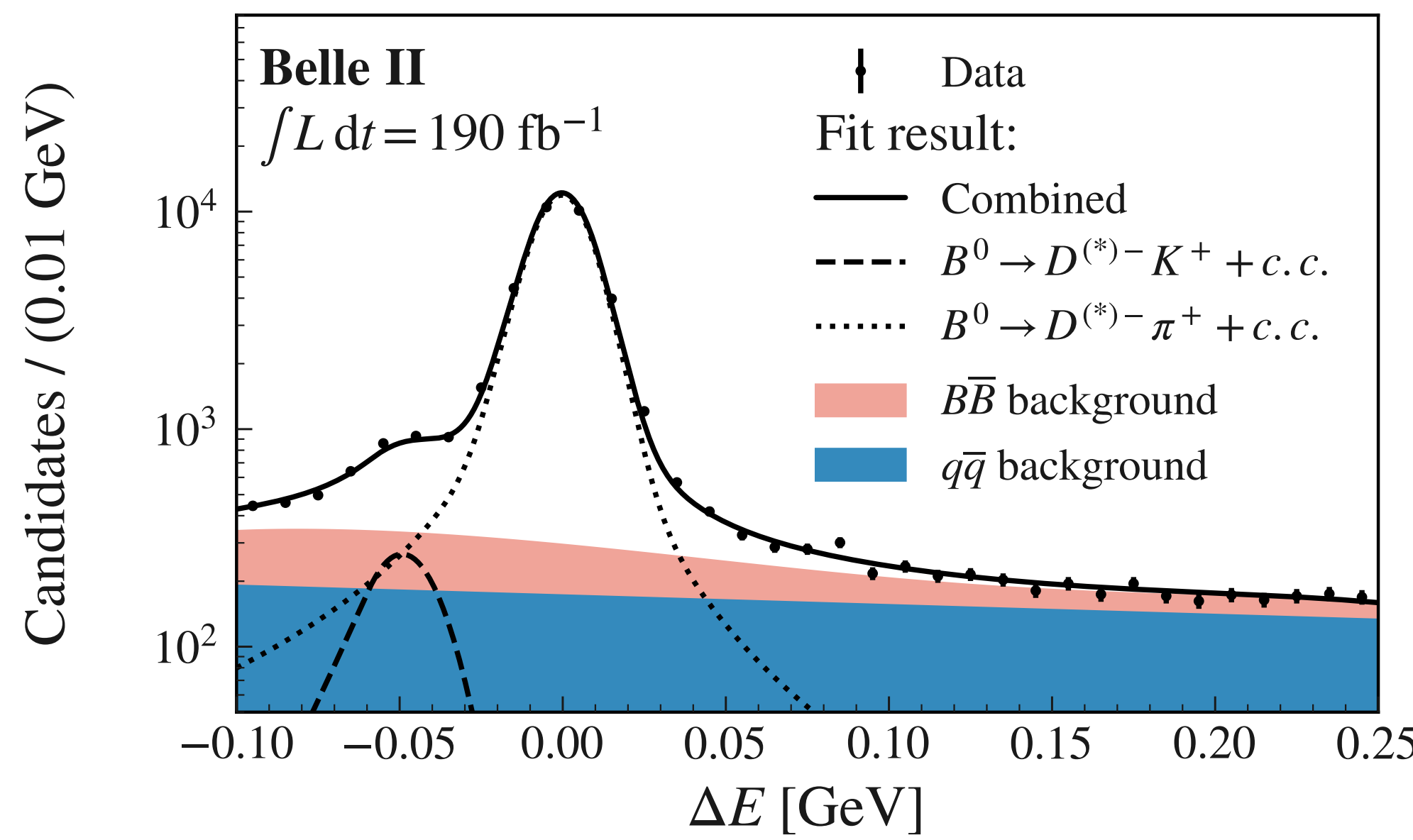
[EPJC 82, 283 \(2022\)](#)



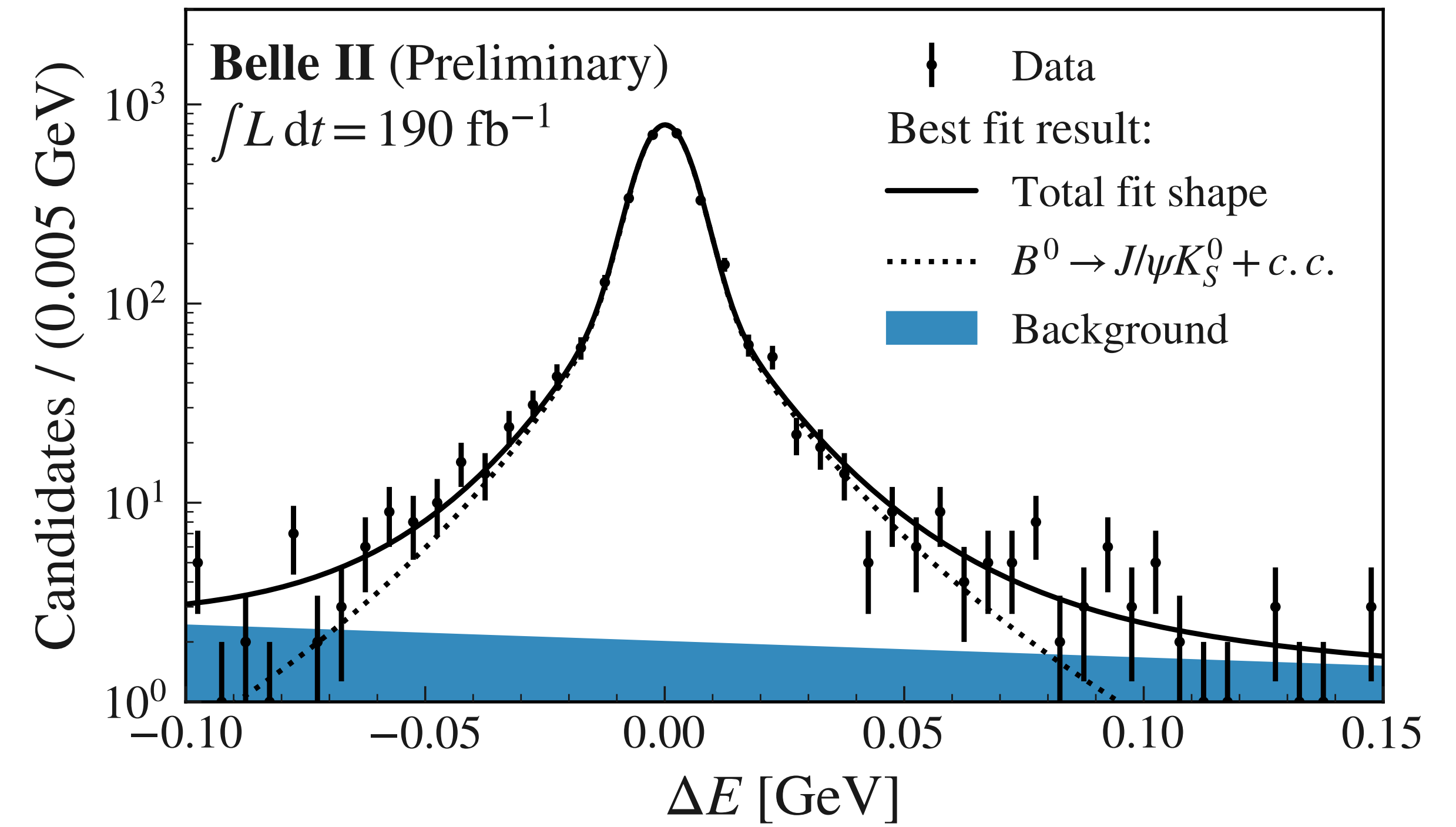
[arXiv:2302.12791](#)



# $B \rightarrow D^{(*)}\pi$

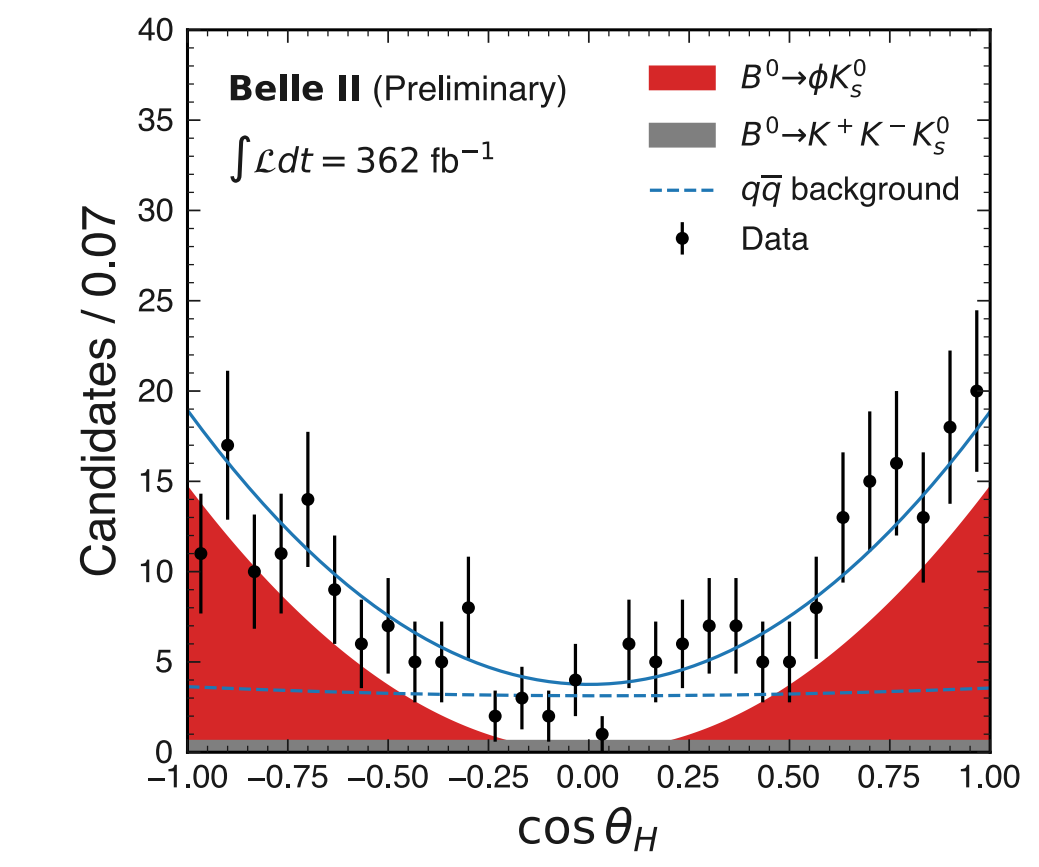
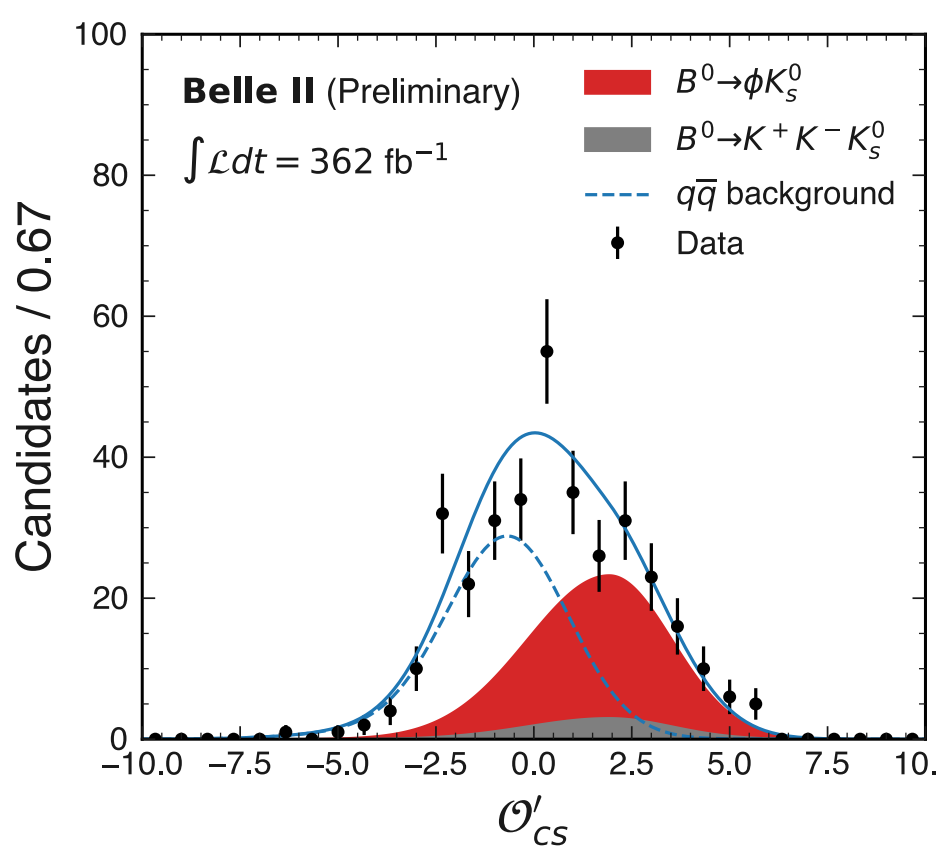
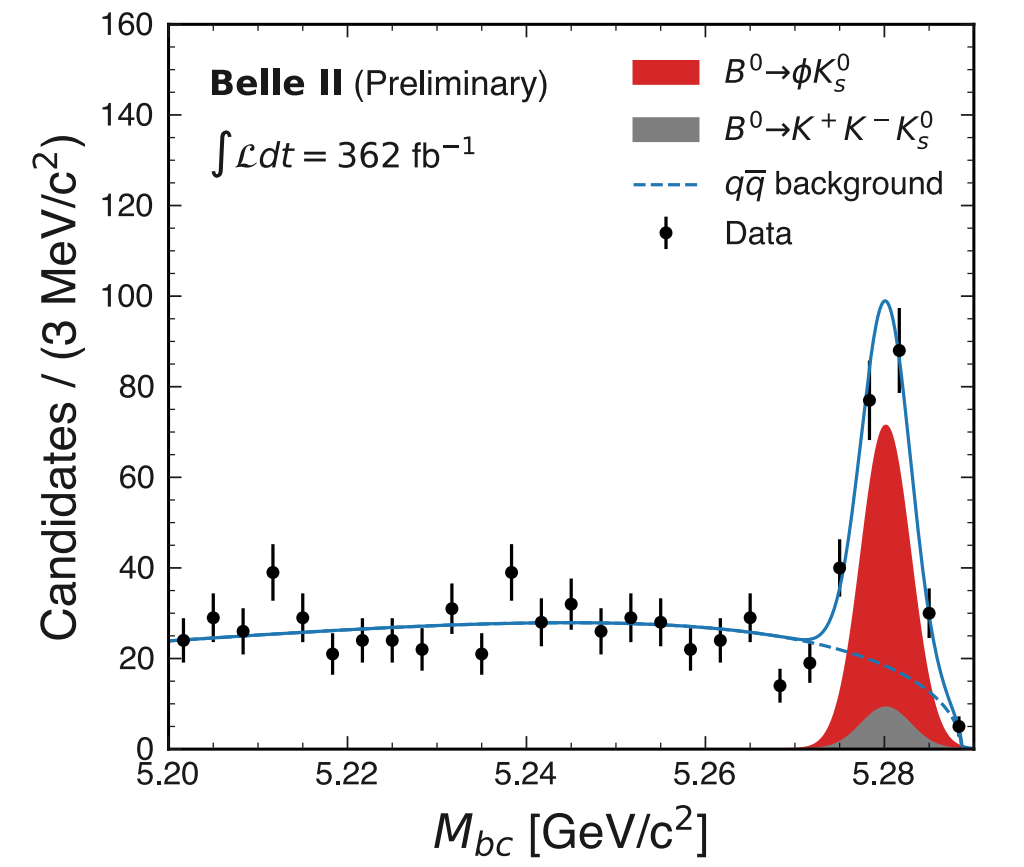


# $B \rightarrow J/\psi K_S$

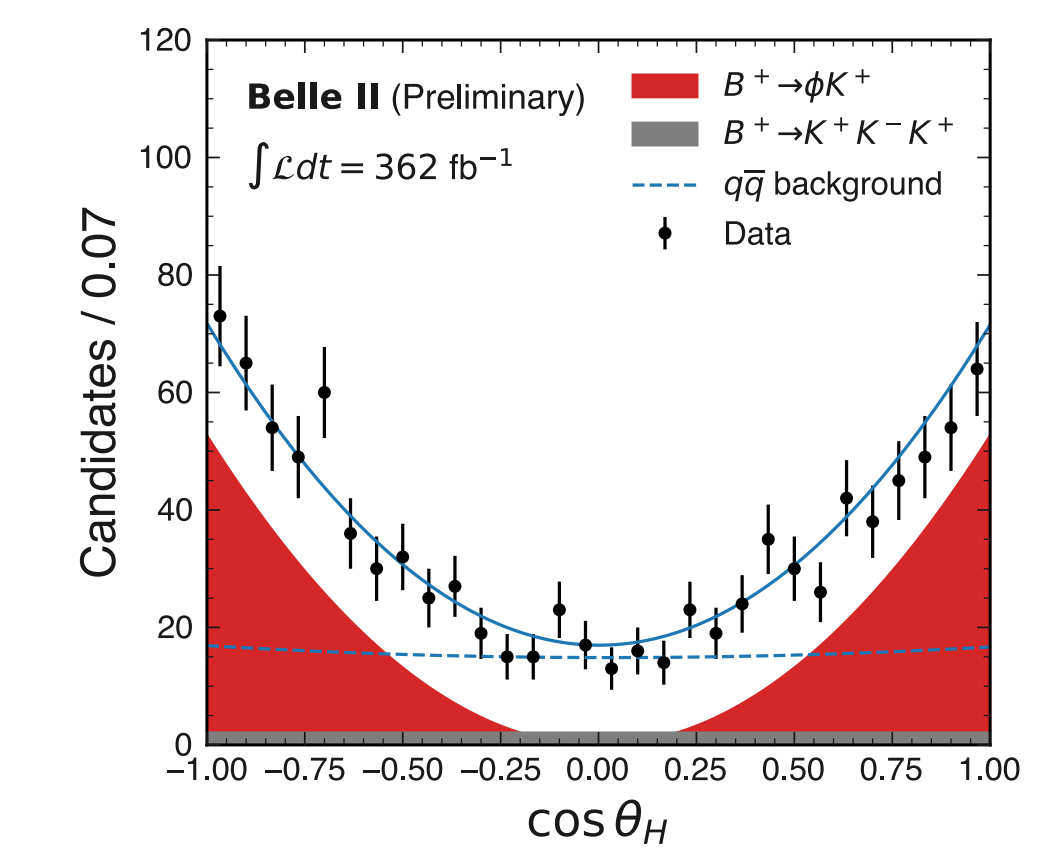
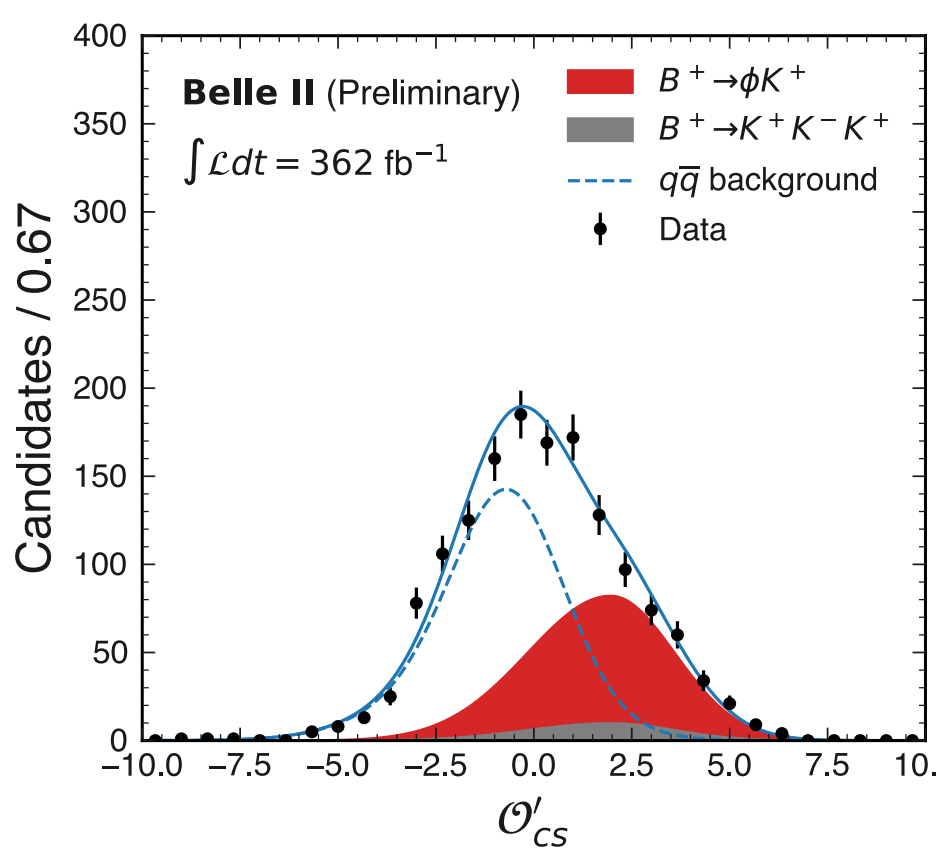
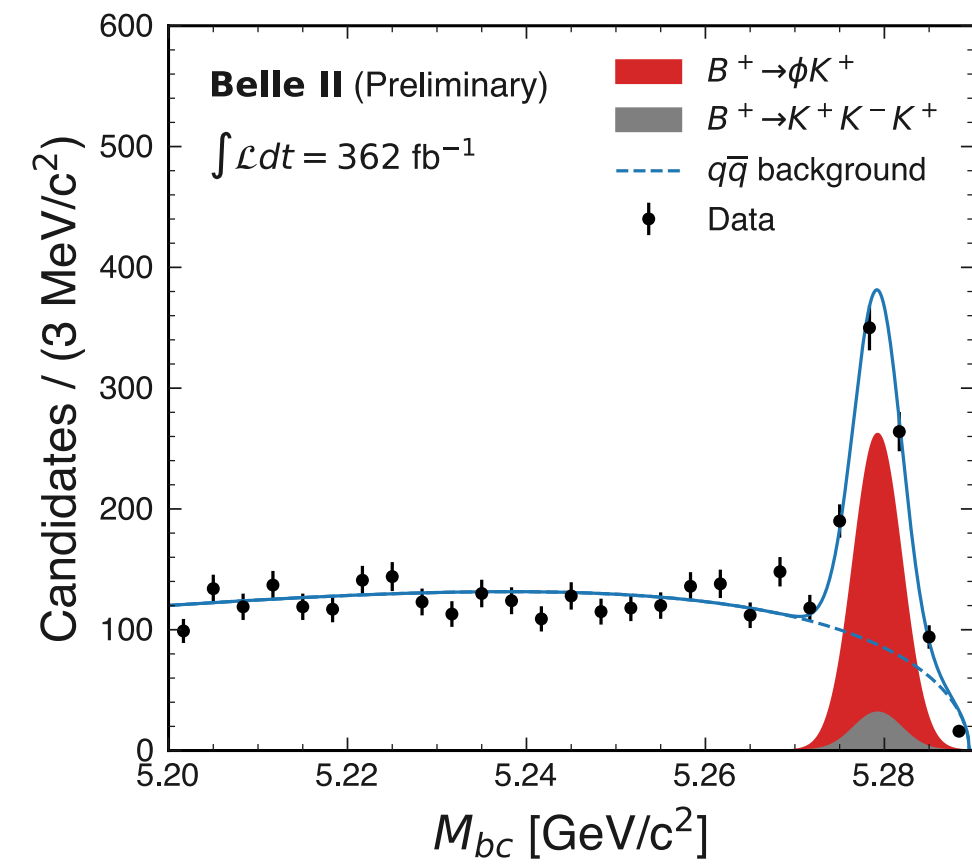


# $B^- \rightarrow \phi K_S$

$B^- \rightarrow \phi K_S$



$B^+ \rightarrow \phi K^+$

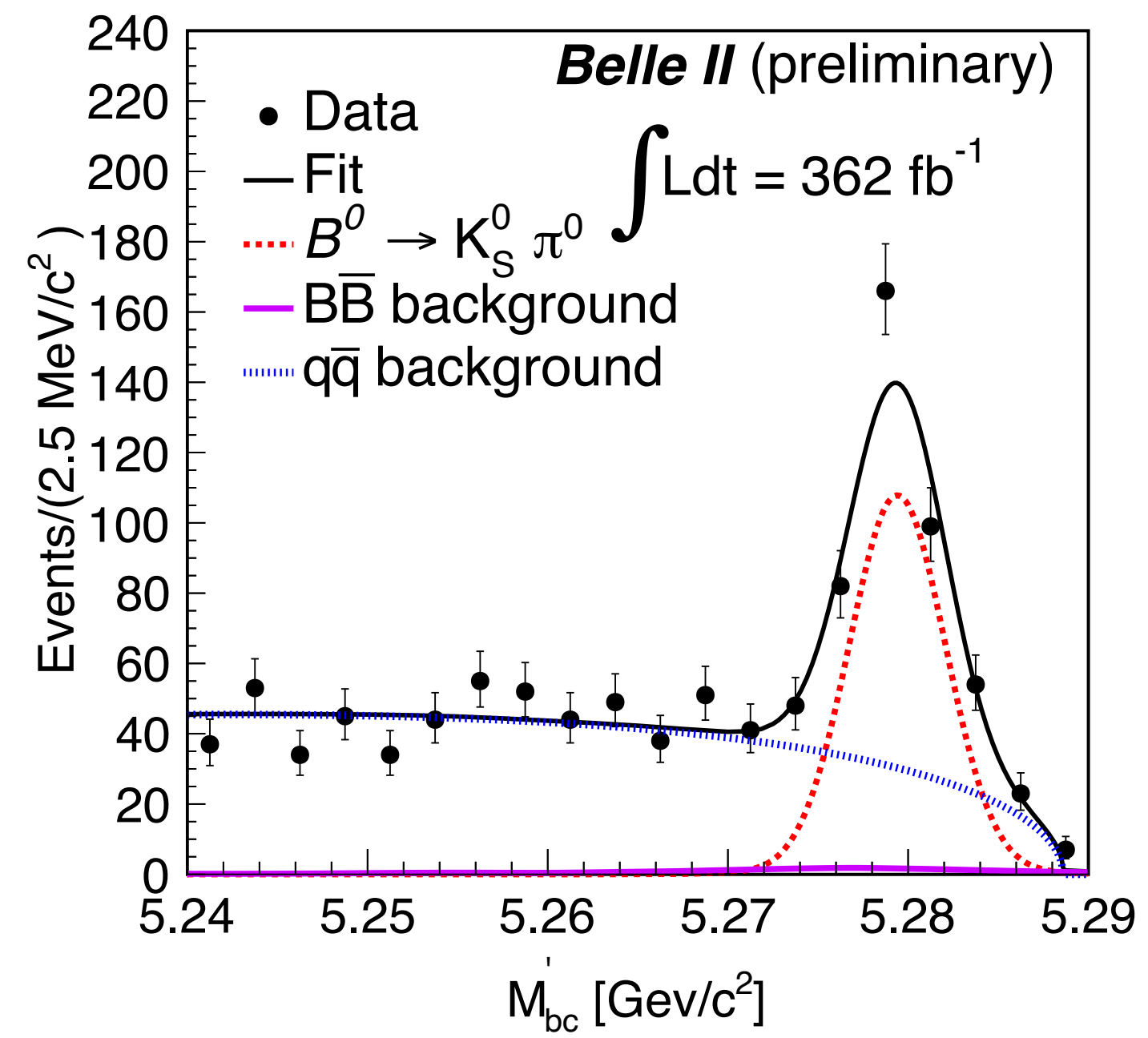


Beam-constrained  
mass

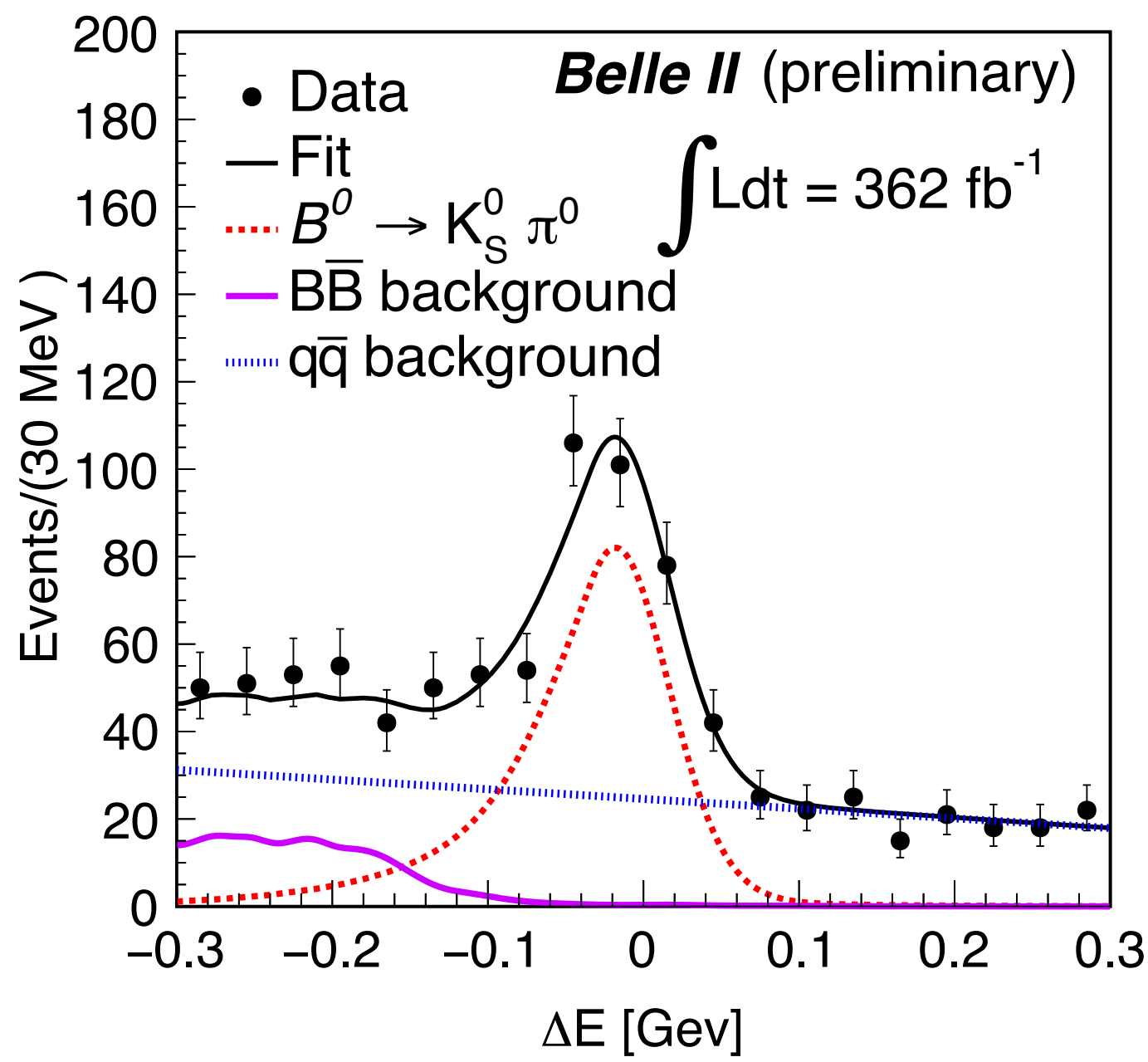
BDT output

Cosine of the  
helicity angle

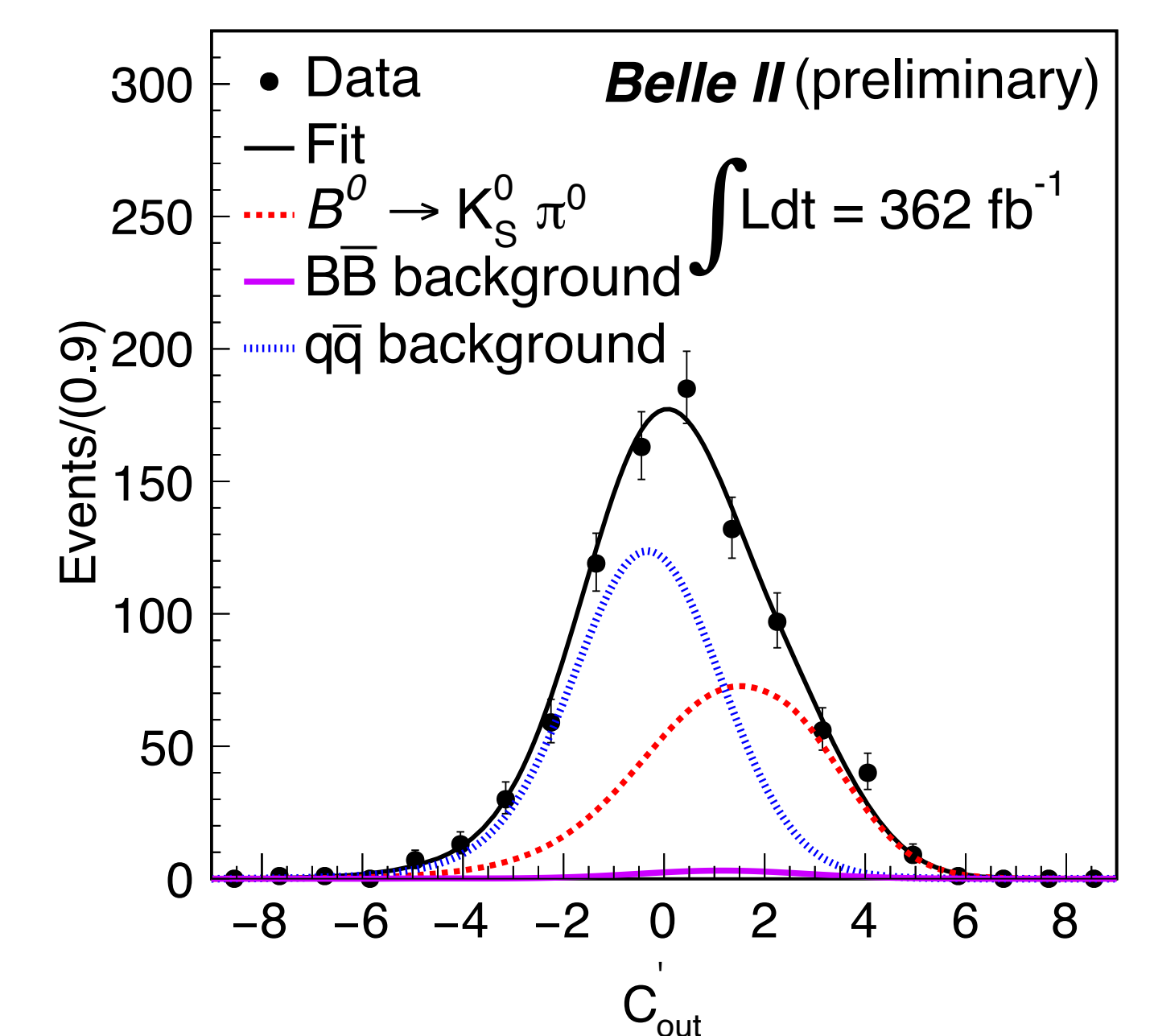
# $B \rightarrow K_S \pi^0$



Beam-constrained  
mass

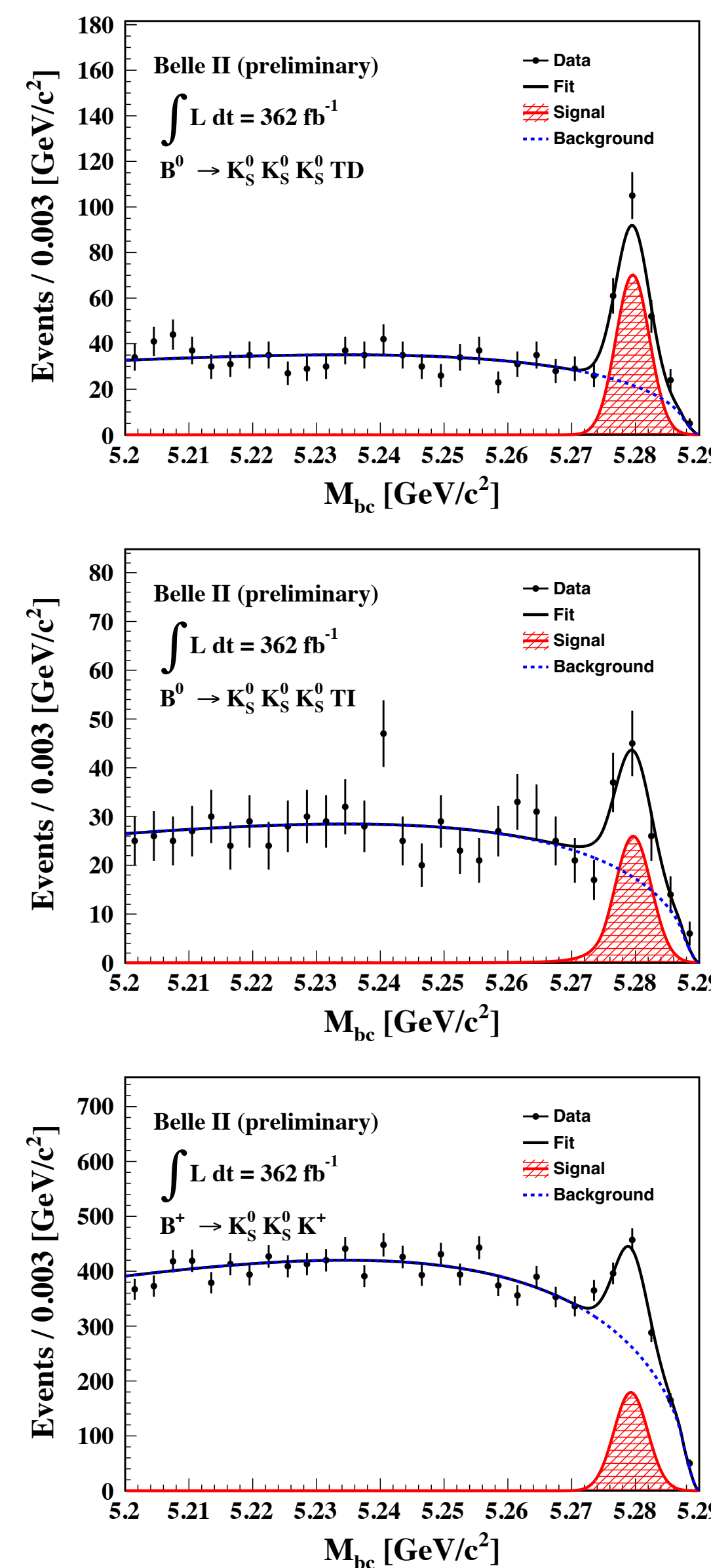


Energy difference

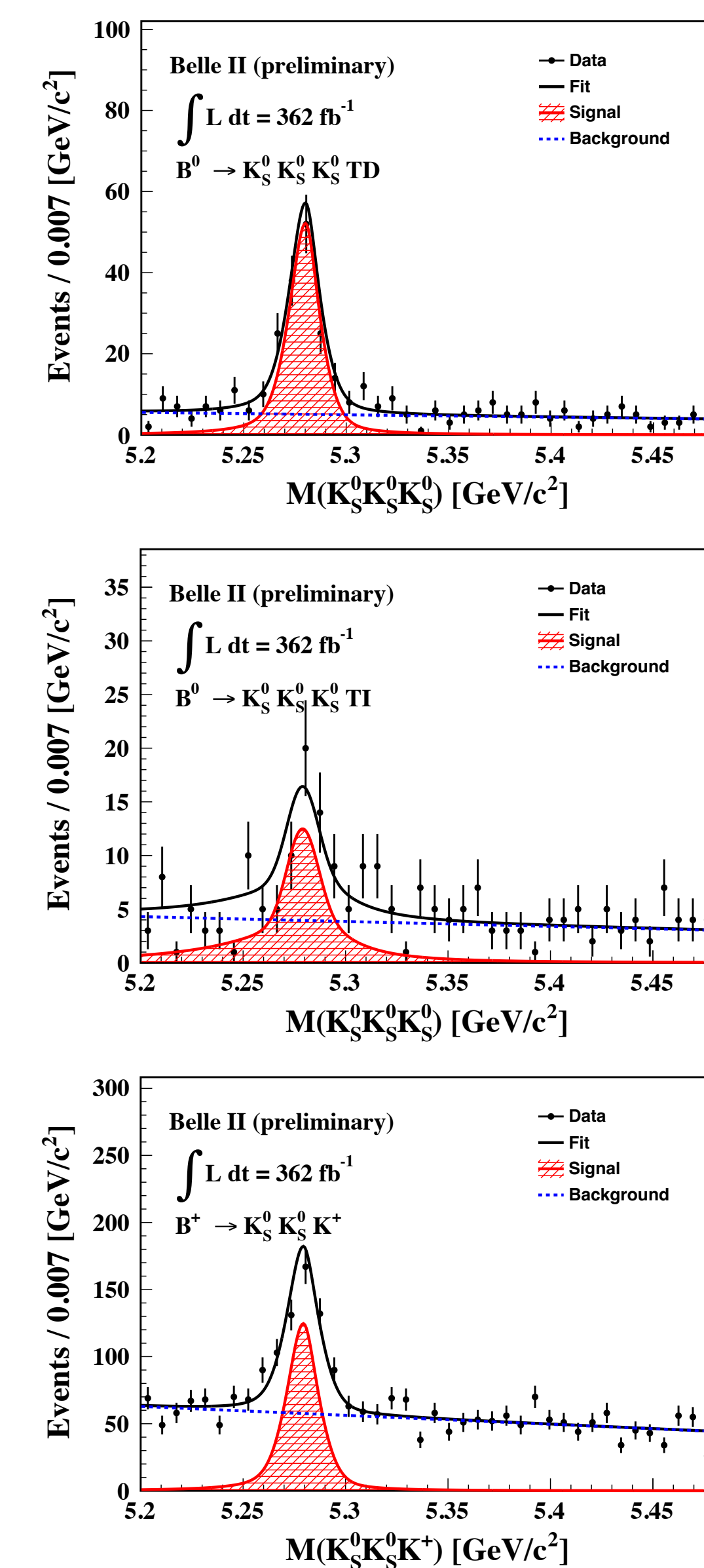


BDT output

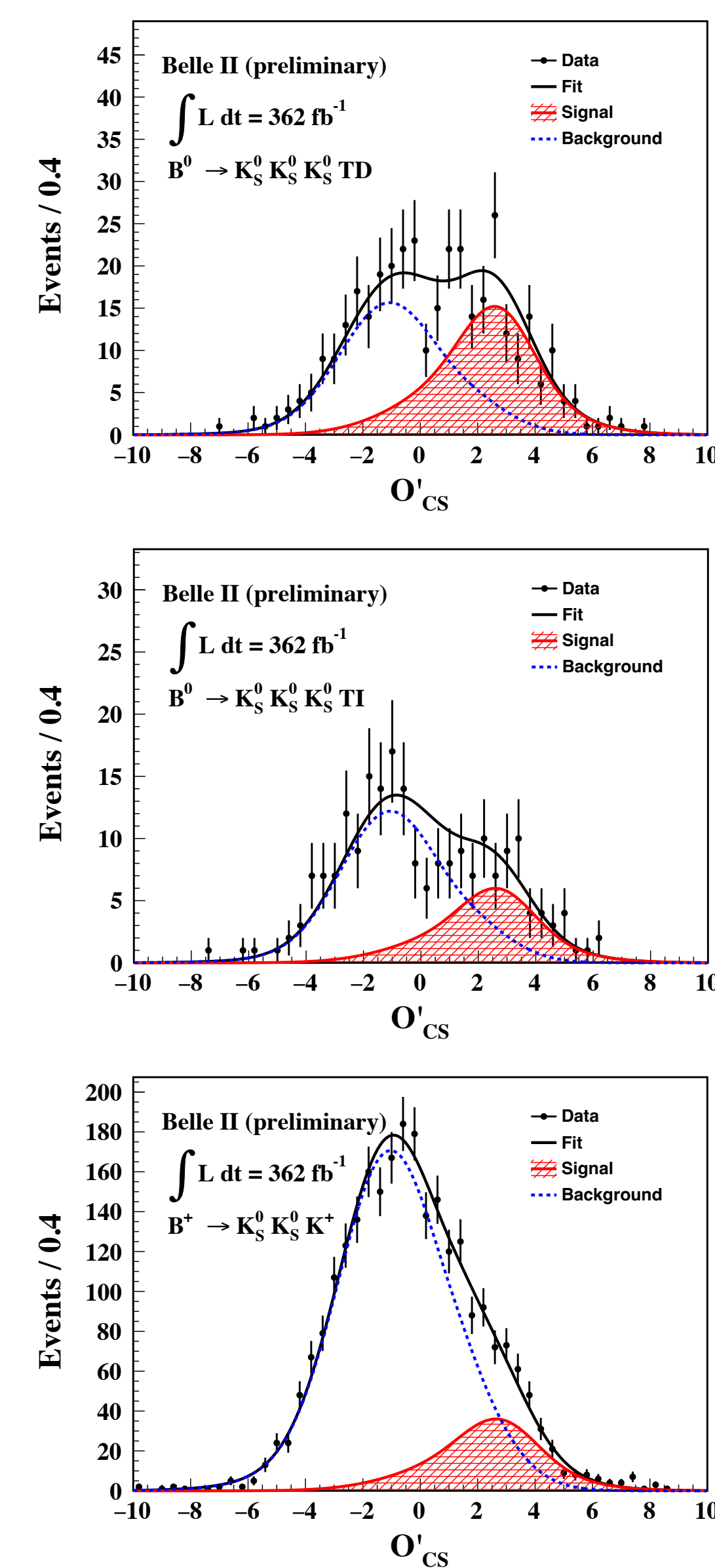
# $B \rightarrow K_S K_S K_S$



Beam-constrained  
mass



Invariant mass



BDT output

TD

TI

$B^+$

# B $\rightarrow$ K<sub>s</sub>K<sub>s</sub>K<sub>s</sub>

